Integrated stochastic reserve estimation and MILP energy planning for high renewable penetration: Application to 2050 South African energy system

Sustainable Energy, Grids and Networks 42 (2025) 101650

Contents lists available at ScienceDirect

Sustainable Energy, Grids and Networks

journal homepage: www.elsevier.com/locate/segan

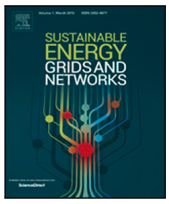

Integrated stochastic reserve estimation and MILP energy planning for high renewable penetration: Application to 2050 South African energy system

Enrico Giglio [a,b,c,e,*], Davide Fioriti [d], Munyaradzi Justice Chihota [e], Davide Poli [d], Bernard Bekker [e], Giuliana Mattiazzo [a,b,c]

[a] Department of Mechanical and Aerospace Engineering, Politecnico di Torino, Corso Duca degli Abruzzi 24, 10129, Torino, Italy
[b] Energy Center Lab, Politecnico di Torino, Via Paolo Borsellino 38/16, 10138, Torino, Italy
[c] Marine Offshore Renewable Energy Lab (MOREnergy Lab), Politecnico di Torino, Via Paolo Borsellino 38/16, 10138, Torino, Italy
[d] Department of Energy, Systems, Territory and Construction Engineering, Università di Pisa, Largo Lucio Lazzarino, 56122, Pisa, Italy
[e] Department of Electrical and Electronic Engineering Stellenbosch University, Banghoek Rd, 7599, Stellenbosch, South Africa

ARTICLE INFO

Keywords:
Power reserve estimation
ENTSO-E
Energy System Modelling
South Africa
Mixed-Integer Linear Programming (MILP)
Resilience
PyPSA

ABSTRACT

The energy transition imposes a shift towards renewable energy sources, and the integration of variable ones introduces significant risks to power system stability. Variable renewable energy sources are mostly unpredictable and can provide limited spare capacity to compensate for imbalance in demand and supply. To meet system adequacy and reliability requirements, the power system is operated with different types of reserve margins to ensure the availability of spare capacity at various time scales. However, despite existing guidelines to operate the current system, limited methodologies have been proposed to estimate reserve requirements for future power systems with high penetration of renewables, including their integration into planning tools. In this study, a comprehensive methodology is proposed to estimate the least-cost power system design which include an endogenous stochastic model for estimating reserve requirements interfaced to a Mixed-Integer Linear Programming model. The proposed stochastic reserve estimation model incorporates generator tripping events, renewable energy variability, and ramping characteristics of the residual demand, extending ENTSO-E guidelines to accommodate future scenarios with high penetration of renewable energy sources. Furthermore, a non-linear parametric function is trained to represent the results of the stochastic reserve estimation model and then integrated into an optimization model to plan future power systems, using an iterative approach. The methodology is validated on the current South African power system. The results indicate the model's effectiveness in optimizing reserve requirements, showing substantial benefits in including storage and other renewable energy technologies to meet future energy demands, while reducing carbon emissions and enhancing grid reliability.

1. Introduction

1.1. Motivation

Accurate planning, management and safe operation of power systems are critical to ensuring their reliability and stability [1]. One way to ensure this is by the procurement of adequate reserve margins both in the short and long-term. However, the increasing integration of renewable energy sources (RES) is challenging the traditional dynamics as they reduce the market profitability of traditional power plants that are also typically involved in providing such reserve margins. As the energy transition demands increasing shares of renewable sources, the need to integrate reserve sizing into energy planning has become significantly relevant [2].

The European Network of Transmission System Operators for Electricity (ENTSO-E) has established robust guidelines for the estimation of the different types of reserve, spatially distributed to ensure the reliable operation of the European regional power system [3]. The current European System Operators adhere to these provisions; yet, the future energy system is demanding significant shift in technologies that requires further investigation, also including the role of storage to serve the different reserve services.

This study builds on the ENTSO-E approach and develops an enhanced comprehensive reserve sizing model (primary, secondary and tertiary) that continues to account for tripping events, while explicitly incorporating variable RES (vRES) penetration, load uncertainty and residual demand variations, which are not explicitly addressed in the

* Corresponding author.
E-mail address: enrico.giglio@polito.it (E. Giglio).

https://doi.org/10.1016/j.segan.2025.101650
Received 12 September 2024; Received in revised form 10 January 2025; Accepted 9 February 2025
Available online 18 February 2025

Nomenclature

Abbreviations

Aux STG	Auxiliary Steam Turbine Generators
BESS	Battery Energy Storage System
CSP	Concentrated Solar Power
DG	Dispatchable Generator
EL	Proton Exchange Membrane Electrolyzer
ENTSO-E	European Network of Transmission System Operators for Electricity
FC	Fuel Cell
HP	Hydropower Plant
PHS	Pumped-Hydro Storage
PV	Photovoltaic
RES	Renewable Energy Source
RMSE	Root Mean Square Error
ToR	Type of Reserve
VRD	Variation of Residual Demand
vRES	Variable Renewable Energy Source
WT	Wind Turbine

Indices and Sets

$\bar{t}$	Indices of snapshots in Monte Carlo simulations domain
Ω_G	Set of DGs
Ω_L	Set of loads
Ω_R	Set of vRES generation techs
Ω_S	Set of storages
Ω_T	Set of timestep t
Ω_{MC}	Set of timestep $\bar{t}$
$\Omega_{R_{rq}}$	Sets of ToR (FCR, aFRR, mFRR, RR)
g	Indices of DGs unit
r	Indices of vRES generation unit
s	Indices of storage units
t	Indices of operating snapshots in MILP optimizations domain

Parameters

$\eta_{s,n}^{ch}$	Charging efficiency coefficients
$\eta_{s,n}^{dsc}$	Discharging efficiency coefficients
$\eta_{s,n}^{sd}$	Self-discharge coefficient
λ_a	Number of failures per year of the ath components
μ_a^{trip}	Tripping probability of the ath components
σ_l	Standard deviation related to forecasting error of lth load
σ_r	Standard deviation related to forecasting error of rth techs
$cc_{a,n}$	Capital costs specific of the ath components
$CF_{r,n,t}$	Capacity factor of rth vRES unit at nth node at tth time step
$e_{s,n,t}^{max}$	Maximum SoC of the sth storage unit
$e_{s,n,t}^{min}$	Minimum SoC of the sth storage unit
$f_{ln,t}$	Power flow in the line lnth at tth time
$K_{ln,n}$	Networks' incident matrix in the line lnth of the nth node
$l_{l,n,t}$	Mean hourly lth load
$oc_{a,n}$	Operational costs specific of the ath components
$p_{a,n,t}^{max}$	Max percentage of power that can be supplied or procured by the ath component at tth timestep
$p_{a,n,t}^{min}$	Min percentage of power that can be supplied or procured by the ath component at tth timestep
sw_t	Weight of the tth snapshot
t_{VRD}	VRS time step

Variables

$d_{a,n,t}$	Mean hourly electrical power supplied or procured at tth time step by the ath component of the nth node
$d_{s,n,t}^{ch}$	Mean hourly charge power of the sth battery
$d_{s,n,t}^{dsh}$	Mean hourly discharge power of the sth storage unit
$e_{s,n,t}$	State-of-Charge of the sth storage at tth timestep
$E_{s,n}$	Nominal capacity (energy) of the sth storage unit
f_{obj}	Objective function
$P_{a,n}$	Nominal capacity (power) of the ath component at the nth node
$R_{rq,\bar{t}}^{\Delta f}$	Power reserve imbalance due to frequency imbalance at $\bar{t}$th timestep in Monte Carlo domain
$R_{rq,\bar{t}}^{imb}$	Total power reserve imbalance at $\bar{t}$th timestep in Monte Carlo domain
$r_{a,n,t}^{ToR}$	Reserve supplied by the ath component at tth time step per each ToR
$R_{rq,\bar{t}}^{trip}$	Power reserve imbalance due to tripping at $\bar{t}$th timestep in Monte Carlo domain
$R_{rq,\bar{t}}^{VRD}$	Power reserve imbalance due to VRD at $\bar{t}$th timestep in Monte Carlo domain
$r_{a,n,t}$	Total reserve supplied by the ath component at tth time step
R_{rq}^{ToR}	Reserve request per each ToR at tth time step
RD_t	Residual demand at tth time step
$s_{a,n,t}$	Status (on/off) of the ath component at tth time step
$u_{a,\bar{t}}$	Availability (on/off) of ath components at $\bar{t}$th timestep in Monte Carlo domain
VRD_t	Variation of residual demand at tth time step
$z_{a,\bar{t}}$	Occurrence (on/off) of fault of ath components at $\bar{t}$th timestep in Monte Carlo domain

original guidelines, to capture dynamics for any present and future energy system. The model will be seamlessly integrated into an electrical system planning framework that includes storage technologies as a reserve source. By extending and refining the ENTSO-E framework, this research enables wider applicability across different countries and anticipates the increased uncertainties associated with future vRES penetration levels.

1.2. Reserve definitions

In power systems, it is crucial to ensure instantaneous balance of demand and supply to maintain system stability, and reserve requirements have been defined accordingly to ensure this secure continuous operation under uncertainties [4]. To achieve this, assets of the power system need to adapt their current operating conditions, upwards or

downwards, in real-time to re-establish the equilibrium and the quality of service [5]. Quick reaction time can be achieved in limited quantity by only few assets that are currently operating with control systems that act proportionally to frequency deviations, as no manual intervention can be fast enough [6]. This high quality reserve band, often referred as primary reserve or Frequency Containment Reserve (FCR) by ENTSO-E, is degraded anytime the frequency of the system does not match the reference value. To ensure the average frequency value is maintained and restored quickly after imbalance events, an additional slower control system under the name of Frequency Restoration is employed, where a distributed signal is sent to selected generation units to change their operation to restore the frequency to the target value [5]. This action involves slower dynamics and some manual interventions may be possible. Specifically, in the ENTSO-E framework [7], the corresponding spare power for frequency restoration is named Frequency Restoration Reserve (FRR) and is distinguished into an automatic (aFRR) and manual (mFRR) shares; the automatic one is also known as secondary reserve. Lastly, to restore the FRR reserve in longer time horizons, further manual actions can be taken to change the operating conditions of the system. The corresponding spare power bands are named Replacement Reserve (RR) or tertiary reserve, compliant to the ENTSO-E format [7,8].

The need for different types of reserve clearly stems from the physical need of guaranteeing the secure balance of the system across time, both in the real-time and short-term, which is why definitions of reserve have been established. Different Transmission System Operators (TSOs) may employ various terminologies for reserves to cover similar operational needs as those reported in the ENTSO-E guidelines [9]. For example, in North America, the Federal Energy Regulatory Commission (FERC) uses terms like Spinning and Non-Spinning Reserve [10]. In the South African power system, reserve requirements categories include Instantaneous Reserve, Regulating Reserve, Ten-Minute Reserve, Emergency Reserve, and Supplemental Reserve, each addressing different timeframes and operational needs [11], which cover the same needs as ENTSO-E but with slightly different constraints. Instantaneous and regulating reserve shall operate within 10 s and be fully activated in 10 min; ten-minute and emergency reserve must be available within 10 min to restore the other reserves. Finally, the supplemental one is the slowest with 6 h delay.

Despite differing names, these reserves address the same physical needs of the power system, as shown in Fig. 1, ensuring rapid response to disturbances and sustained balancing over time.

To summarize the reserve types within the ENTSO-E framework:

- FCR (primary reserve) is activated immediately after an imbalance event, e.g. the tripping of a large generator, to restore supply–demand balance (approximately 30 s to be fully available).
- aFRR (secondary reserve) is activated slightly after FCR to help restoring frequency and power balance (approximately 5 min to be fully available).
- mFRR and RR (tertiary reserve) are engaged subsequently to aFRR (approximately 12.5–15 and 30–45 min to be fully available), contributing further to maintaining system balance and stability.

These categorizations ensure a comprehensive approach to managing power system stability, accommodating both immediate and prolonged balancing needs. Although based on ENTSO-E guidelines, the nomenclature reflects the similar operational requirements of TSOs globally, ensuring the approach is applicable beyond the specific ENTSO-E context and, for this reason, has been used as reference for this paper.

1.3. Techniques for reserve estimation

Different techniques have been proposed to quantify how much reserve by type shall be guaranteed to ensure an acceptable level of security of the system. The primary reserve (FCR) is typically determined using a deterministic approach based on historical data and worst-case scenarios [12] in order to ensure an immediate response to frequency deviations. The secondary (aFRR) and tertiary (mFRR and RR) reserves use a combination of empirical methods and probabilistic approaches [13]. The empirical methods are based on peak load values and historical data, while the probabilistic approaches incorporate variables such as plant outages, load variations, forecast errors and exchange schedules to calculate reserve requirements with a high level of statistical confidence [14]. Authors in [15,16] extended the ENTSO-E framework to scenarios with a high penetration of vRES and the inclusion of storage technology in the power reserve supply. Their models included the integration of primary reserves, assuming a fixed value of 3000 MW for the European area, and focused on improving the methodologies for secondary and tertiary reserves with high vRES levels. However, these studies adopted fixed values for primary reserve, neglected the impact of ramps and asset tripping into the reserve, and the modelling of tertiary reserve does not extend across multiple time horizons.

The North American Electric Reliability Corporation (NERC) has traditionally emphasized a static reserve requirement, where reserve values are predefined and only adjusted for specific times of day or conditions [6]. However, recent studies suggest the need for dynamic reserve requirements that respond to real-time system conditions, particularly with the increasing penetration of vRES such as wind and solar [17].

The authors of [14] have developed a comprehensive methodology for estimating secondary and tertiary reserve requirements based on data-driven approaches for the current power system. This methodology, tested in Northern Italy for the current system, is in line with ENTSO-E and Italian TSO (Terna) guidelines [18] and provides detailed calculations for spinning and non-spinning reserves. However, this approach does not incorporate future scenario planning nor primary reserve estimation, indicating an area for further research and development. Additionally, while the methodology considers load forecast errors and integrates the effect of residual load variation in the calculation of tertiary reserve needs, it is modelled for a maximum duration of one hour, which may not fully capture the requirements for longer-term stability provided by RR. This highlights the need for a more extended reserve duration model and the inclusion of RR to ensure comprehensive system reliability.

Reserve estimation methodologies vary significantly across regions and contexts. According to the literature and to the best of the authors' knowledge, various techniques have been proposed, but there is a gap in dynamic reserve quantification methodologies that extensively model uncertainty and are applicable to future power systems capacity planning with varying degrees of vRES penetration. Existing techniques are generally derived from standard practices and focus on the operation of current systems, as such their acceptability to significantly different future systems has yet to be validated. That is why it is deemed useful in this study to provide a consistent statistical framework to probabilistically estimate the non-linear reserve requirements for any system configuration and customizable levels of risk.

1.4. Reserve requirements in power system planning

Incorporating reserve requirements into power system planning is crucial for maintaining long-term system reliability, especially with the increasing integration of vRES. Several studies have integrated reserve estimation into energy planning models, but significant gaps remain in addressing all necessary aspects comprehensively.

The authors in [16] extended the ENTSO-E framework to include high vRES scenarios and the planning of storage and vRES technologies. Their model allowed for storage technologies to balance supply and demand and to provide reserve capacities. However, as highlighted in the previous section, it presents gaps in the model for reserve

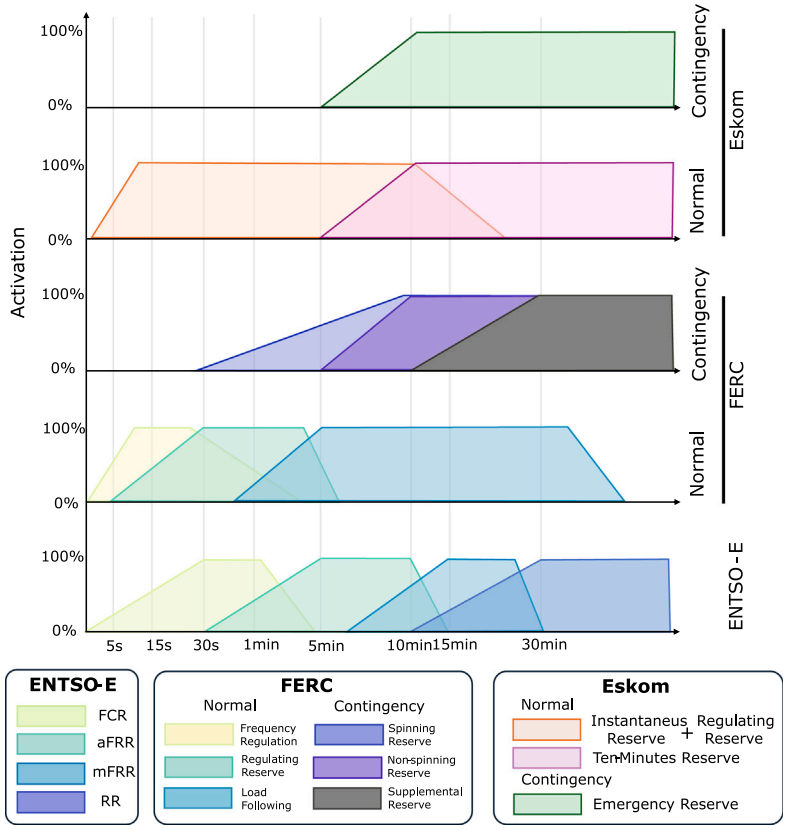

Fig. 1. Graphical comparison between the different types of reserve under the different definitions. Inspired by [10].

estimation, particularly in dynamically adjusting primary reserves and fully integrating the impacts of generation tripping events and residual demand variation effects.

The study in [19] proposed the H2RES model to analyse the impact of demand response and reserves on long-term energy planning for small islands. While it emphasized primary and secondary reserves, their requirements were hard-coded and lacked a statistical framework. Additionally, the model did not account for reserve needs due to variations in residual demand (VRD), critical for managing supply and demand fluctuations.

The study in [20] addresses both planning and operational constraints, emphasizing the need to integrate operational flexibility into generation planning, including dynamic reserve requirements that respond to real-time conditions. However, this study does not fully address the probabilistic nature of vRES variability and does not consider tripping events in generation components.

It is worth noting that in the existing literature, and to the best of the authors knowledge, no other paper addresses these gaps by developing a comprehensive methodology for estimating all types of reserves through a non-linear stochastic approach that is efficiently incorporated into an energy planning model.

1.5. Novelty and contribution

The novelty of this work lies in the development of (a) an open-source general methodology to estimate reserve needs for arbitrary future power needs and (b) an integrated planning model that incorporates variegated reserve needs within the optimization. This model uses a stochastic approach for estimating different types of reserves, building on and extending the ENTSO-E guidelines to accommodate high penetration of RES. The model is also applied to the case study of South Africa, a country experiencing significant load shedding, compounded by an aging and unreliable coal fleet with complex tripping characteristics. This high uncertainty context, coupled with significant potential for vRES [21], makes traditional techniques to estimate reserve requirements unsuitable [22]. Furthermore, the proposed case study selected demonstrates the feasibility and generalizability of our approach beyond the initial scope of ENTSO-E guidelines. Key innovations of the paper include:

- comprehensive non-linear stochastic model to estimate reserve requirements, considering tripping phenomena of system components, forecasting uncertainties and variability of vRES and load, and the effect of VRD;
- approach to efficiently linearize the non-linear reserve requirements to adapt to arbitrary future energy systems configurations;
- open-source development of an iterative integrated planning technique that optimally sizes the system accounting for non-linear reserve requirements [23];
- application of the entire procedure to the South African power system, validated against the actual system operation, where, according to the literature analysis and to the best of the authors' knowledge, no integrated energy planning approach with a stochastic reserve estimation has yet been presented.

This comprehensive approach ensures a robust and reliable estimation of power reserves in future energy scenarios with significant vRES integration.

1.6. Structure of the work

The structure of this work is as follows. First, the proposed integrated model is presented (Section 2), focusing initially on the stochastic model for reserve estimation and the linearization of reserve requirements (Section 3), followed by the MILP problem for energy system planning (Section 5). Subsequently, Section 6 introduces the South African case study, defining the domain for the MILP problem and providing a validation of the techno-economic assumptions for this

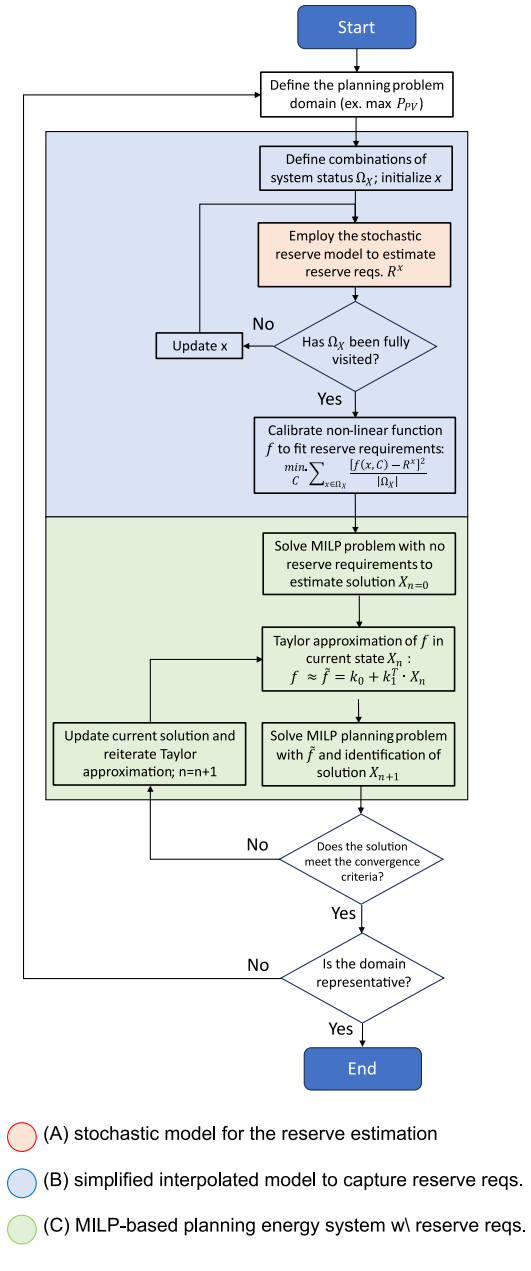

Fig. 2. The optimization algorithm.

context. Then, in Section 7, the stochastic model for reserve estimation is applied to the South African power system, and the results are presented and discussed. Finally, Section 8 provides conclusions on the proposed methodology and highlights the qualitative contribution offered by the chosen case study.

2. The comprehensive planning model under uncertainties

This section presents the proposed integrated optimization algorithm, shown in Fig. 2, that is composed by three main parts: (A) a stochastic model for the reserve estimation, (B) a simplified interpolated model to capture reserve requirements, and (C) a MILP-based planning energy system including reserve requirements.

The stochastic reserve estimation model (A) is responsible for generating the reserve requirements needs for a given set of operating assets, their set point, the load, and the corresponding variation in residual demand. The methodology performs Monte Carlo simulations to generate tripping scenarios of generation and converter assets, extract uncertainties in the demand and variable renewable sources and models the effect of VRD to estimate the reserve needed for any given configurations. Once the scenarios are complete, they are statistically characterized and the desired level of reserve is selected to satisfy an acceptable level of risk. This robust approach is general and can be applied to calculate the reserve needs at any operating conditions of a system. However, it cannot be coupled as-is to large-scale energy system planning as it is highly non-linear and time-step specific, which makes it difficult to be coupled with planning tools. Therefore, a parametric fitting approach based on a non-linear function is proposed in the second step (B) to enable the stochastic reserve model developed in (A) to be coupled with the proposed planning model described in (C), by linearizing the non-linear function. The stochastic model for the reserves estimation is detailed in Section 3.

The second step (B) makes use of the stochastic reserve model developed in (A) to calibrate a simplified non-linear parametric model that approximates the need for reserve for any configurations of the system. This intermediate step enables creating a reserve model that is possible to interface to the MILP planning model (see Section 5.7). Please note that as the reserve needs are non-linear, a linearization is needed, as discussed in the subsequent step.

The last part (C) employs a MILP optimization model to optimally size the energy system, while accounting for the reserve requirements (as detailed in Section 5). The MILP model accounts for the detailed representation of the different reserve needs for the system and the reserve models previously discussed. In particular, as the reserve needs are non-linear, an iterative linearization process is performed. In every iteration, the reserve model developed in (B) is linearized using Taylor approximation given the results of the previous iteration, and the results are employed to define the reserve needs. Then, the optimization is solved again and the iterations are repeated until convergence.

3. Stochastic model for the reserve estimation

3.1. Description

The proposed probabilistic approach for reserve dimensioning aims to account for the major sources of power imbalances, namely:

- Tripping events of power generation components (generators and storage power converters, such as inverters) and/or major power lines. For every tripping event, the imbalance to be covered by reserve assets is expected to last for a given time (t_{OFF} assumed to be 30 min [7]).
- Forecasting errors related to loads and vRES generation, i.e. the discrepancy between the predicted power and the actual measured power in a specific area of an electrical system, considering their average value at minute level resolution.
- The variation in the power supplied by dispatchable generators (DGs) due to increases in the residual demand between two time steps. As the markets operate at discrete intervals, usually with 15- or 60-min resolution, the average value of the interval can hide a upward (or downward) ramping event that increases the need for demand within the interval that needs to be considered.

To achieve this, a Monte Carlo procedure is proposed (illustrated in Fig. 3) to estimate all reserve requirements in agreement with ENTSO-E nomenclature (Fig. 1).

Similarly to the ENTSO-E methodology [13], for any system configuration, we propose to simulate the 1-min operation of that configuration for a large enough time horizon $\bar{t} \in \Omega_{MC}$ (equivalent to an horizon of 192 years) to reliably extrapolate the needs for reserve using statistical properties [7]. A 192-year horizon corresponds to 10^8 time steps for each Monte Carlo simulation, ensuring the capture of at least 100 trips for a component with a failure rate of about 10^{-6}, which is the lowest value among components to the best of the authors'

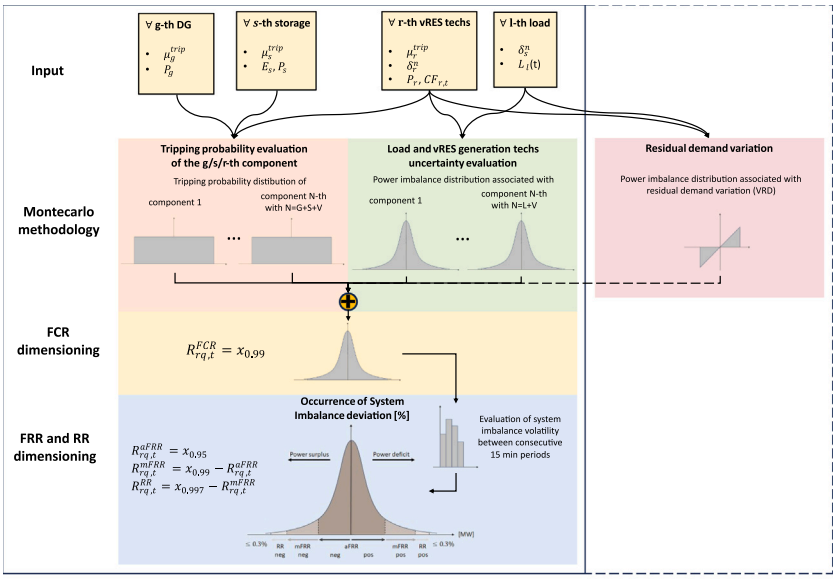

Fig. 3. The stochastic methodology adopted to size the reserve requirements function.

knowledge [24]. The requirements for FCR, aFRR, mFRR and RR are calculated according to three pre-set percentiles, similarly to [13]. The Monte Carlo technique is employed to generate the whole imbalance scenario and then the percentiles are calculated. The tripping model of generators assumes a constant tripping probability and the contribution of the trip event to the reserve lasts for t_{OFF} period, which corresponds to 30 min. The choice of 30 min, according to ENTSO-E guidelines [7], is based on the consideration that the unit that tripped will not be reconnected and partially compensate the imbalance it has caused within the time of deployment of FRR. The uncertainty in the load and renewable sources shall be calibrated using real data and when unavailable, the Gaussian probabilistic model is assumed, in agreement with the literature [15].

3.2. Monte Carlo model

3.2.1. The general model

The Monte Carlo model aims to reproduce the statistical properties of the imbalances experienced by the power systems described above. Accordingly, we model the total system imbalance $R^{imb}_{rq,\bar{t}}(\mathbf{x})$ in (1) as composed by three terms: the tripping of assets $R^{trip}_{rq,\bar{t}}$, the forecasting uncertainties $R^{\Delta f}_{rq,\bar{t}}$ and effect of VRD $R^{VRD}_{rq,\bar{t}}$, for every time step $\bar{t} \in \Omega_{MC}$ of the Monte Carlo procedure. The details of the different terms are highlighted in the progressing discussion, yet note how the total unbalance along the different time steps $\bar{t}$ in the Monte Carlo domain depends on the specific combination $\mathbf{x}$ of the considered equipment. Each combination $\mathbf{x}$ is uniquely determined by the nominal power per the different components P_a (which affect the tripping unbalances), a value of the total load $\sum_{l\in\Omega_L} L_l$ and vRES generation $\sum_{r\in\Omega_r} P_r \cdot CF_r$ (which affects $R^{\Delta f}_{rq,\bar{t}}$) and the VRD. It follows that each Monte Carlo simulation refers to a single scenario of load and vRES generation, and then its results could potentially be considered for a limited number of snapshots of the energy system that will be optimized in the following step of the general model (see Section 5).

$$R^{imb}_{rq,\bar{t}}(\mathbf{x}) = R^{trip}_{rq,\bar{t}}(\mathbf{x}) + R^{\Delta f}_{rq,\bar{t}}(\mathbf{x}) + R^{VRD}_{rq,\bar{t}}(\mathbf{x}), \quad \mathbf{x} = \{P_a, \dots, CF_r, \dots, L_l, \dots, VRD\} \tag{1}$$

$R^{imb}_{rq,\bar{t}}$ is necessary to estimate the real-time imbalances needed to appropriately estimate FCR. However, as FRR and RR occur at slower dynamics that smooth the imbalance requirements, it is useful to define the residual imbalance $R^{\Delta imb}_{rq}$ as shown in Eq. (2), which is $R^{imb}_{rq,t}$ deprived of its average component computed across the market time step (every 15 min). While FCR will be sized according to $R^{imb}_{rq,t}$, the other reserve categories are sized according to $R^{\Delta imb}_{rq,t}$, as later clarified.

$$R^{\Delta imb}_{rq,\bar{t}}(\mathbf{x}) = R^{imb}_{rq,\bar{t}}(\mathbf{x}) - \frac{\sum_{\bar{t}^*=t_0}^{t_0+15} R^{imb}_{rq,\bar{t}^*}(\mathbf{x})}{15}, \quad t_0 = \left\lfloor \frac{\bar{t}}{15} \right\rfloor \tag{2}$$

3.2.2. Tripping of assets

The reserve requirement due to trip events is calculated as shown in Eq. (3), where $u_{a,\bar{t}}$ is a set of binary variables indicating the ongoing impact of a tripping event of the asset a for the current Monte Carlo's time step $\bar{t}$, P_a is the nominal capacity of the asset and CF_r is the capacity factor. It is worth noticing that although the trip events are instantaneous and occur in specific time steps, their reserve impact last multiple time steps (t_{OFF}). To simulate that, Eq. (5) generates a uniformly distributed random variable Z that triggers the trip event when its value exceeds the trip probability μ^{trip}_a, and $z_a(\bar{t})$ becomes positive. Then, the impact of the trip event is prolonged by t_{OFF} time, using (4). Finally, the tripping probability is modelled as an exponential distribution shown in (6), where λ_a is the number of failures per year.

$$R^{trip}_{rq,\bar{t}}(\mathbf{x}) = \sum_{a\in\Omega_G\cup\Omega_S} u_{a,\bar{t}} \cdot P_a + \sum_{r\in\Omega_R} u_{r,\bar{t}} \cdot P_r \cdot CF_r \tag{3}$$

$$u_{a,\bar{t}} = \begin{cases} 1 & \exists \hat{\bar{t}} \in [\bar{t} - t_{OFF} - 1, \bar{t}) : z_{a,\hat{\bar{t}}} = 1 \\ 0 & \text{otherwise} \end{cases} \tag{4}$$

$$z_{a,\bar{t}} = \begin{cases} 1 & Z > \mu^{trip}_a, \quad Z \sim U[0,1] \\ 0 & \text{otherwise} \end{cases} \tag{5}$$

$$\mu^{trip}_a = 1 - e^{\lambda_a}, \quad a \in \Omega_G \cup \Omega_S \cup \Omega_R \tag{6}$$

3.2.3. Forecasting uncertainties

The contribution to the imbalance due to zero-sum uncertainties $R^{\Delta f}_{rq,t}$ is modelled in (7) as a generic distribution function f that is a function of the demand $L(t)$, the installed capacity P_a, and capacity factors $CF_r(t)$ of vRES.

$$R^{\Delta f}_{rq,\bar{t}}(\mathbf{x}) \sim f(\mathbf{x}), \quad \forall \bar{t} \in \Omega_{MC} \tag{7}$$

As error distributions naturally tend to behave as Gaussian distributions [15,16], this study proposes a specific approximation where uncertainty distributions are assumed to be Gaussian. The total standard deviation of the frequency deviation $\sigma_{\Delta f}(\mathbf{x})$ is calculated as shown

in Eq. (8), where σ_l and σ_r are the standard deviation of the lth loads L_l and rth vRES techs P_r.

$$\sigma_{\Delta f}(\mathbf{x}) = \sqrt{\sum_{l\in\Omega_L} \sigma_l^2 \cdot L_{l,ref} \cdot L_l + \sum_{r\in\Omega_R} \sigma_r^2 \cdot P_{r,ref} \cdot P_r \cdot CF_r} \tag{8}$$

Eq. (9) models the reserve requirement due to forecasting errors.

$$R^{\Delta f}_{rq,\bar{t}}(\mathbf{x}) \sim N[0, \sigma_{\Delta f}], \quad \forall \bar{t} \in \Omega_{MC} \tag{9}$$

3.2.4. Impact of variation of residual demand

Finally, the contribution of the VRD within each market interval (generally 15–60 min) is modelled as a saw-tooth wave function as described in (10) with slope A^{VRD} proportional to the VRD. Eqs. (11)–(37) denote the numerical expression of the terms. In the application of our model, t_{VRD} is assumed equals to 15 min.

$$R^{VRD}_{rq,\bar{t}}(\mathbf{x}) = A^{VRD} \cdot 2 \cdot \left(\frac{\bar{t}}{t_{VRD}} - \left\lfloor \frac{\bar{t}}{t_{VRD}} + \frac{1}{2} \right\rfloor \right) \tag{10}$$

$$A^{VRD} = \frac{VRD}{\frac{1\text{h}}{t_{VRD}} \cdot 2} \tag{11}$$

3.3. Reserve requirements by type

Upon completion of the Monte Carlo simulation, FCR, aFRR, mFRR and RR reserve requirements are defined similarly to the ENTSO-E guidelines [13,15], as shown in (13)–(15), respectively, where function $PC_p(D)$ computes the percentile p of distribution D.

$$R^{FCR}_{rq}(\mathbf{x}) = PC_{.997}(R^{imb}_{rq,\bar{t}}(\mathbf{x})) \tag{12}$$

$$R^{aFRR}_{rq}(\mathbf{x}) = PC_{.95}(R^{\Delta imb}_{rq,\bar{t}}(\mathbf{x})) \tag{13}$$

$$R^{mFRR}_{rq}(\mathbf{x}) = PC_{.99}(R^{\Delta imb}_{rq,\bar{t}}(\mathbf{x})) - R^{aFRR}_{rq}(\mathbf{x}) \tag{14}$$

$$R^{RR}_{rq}(\mathbf{x}) = PC_{.997}(R^{\Delta imb}_{rq,\bar{t}}(\mathbf{x})) - R^{mFRR}_{rq}(\mathbf{x}) \tag{15}$$

4. Non-linear reserve parametrization for planning purposes

4.1. Non-linear model

As reserve requirements must be satisfied for every time step of the simulation, the model described in the previous section is too complex to be included as-is within planning optimization problems. Therefore, this section proposes a methodology to approximate the overall complex model using a (non-linear) analytical function $f(\mathbf{x})$ to approximate the reserve requirements of a system status $\mathbf{x}$. As analytical functions are easier to handle by optimization tools, this step is a key element for the successful interface of the stochastic reserve model with optimization planning tools. The proposed process to calibrate this non-linear function involves the following steps:

- Define the shape and arguments of the non-linear function $f(\mathbf{x}, C)$ that approximates the reserve needs, where C are the fitting parameters and $\mathbf{x}$ are the independent variables. Examples of variables are the number, type, and nominal power of generating components online, vRES penetration, loads, and variations in residual demand, that are also the main input parameters to the stochastic reserve model described in Section 3.
- Define the set Ω_x of combinations of parameters to train the approximate model. Examples of parameters are tripping scenarios, vRES penetration levels, and VRD variations.
- Calculate the reserve R^x needs for any defined combination $x \in \Omega_X$ of parameters defined in the previous step, using the full implementation of the stochastic model for reserve quantification. This process aims to define the reserve values to be used for the fitting of the proposed (non-linear) function f.
- Determine the coefficients C of the non-linear function to best approximate the reserve needs for each type of reserve (FCR, aFRR, mFRR, and RR). For each reserve requirements, the square error in (16) is minimized.

$$\min_C \sum_{\mathbf{x}\in\Omega_X} \frac{\left[f(\mathbf{x}, C) - R^x\right]^2}{|\Omega_X|} \tag{16}$$

For the purpose of this study, but with no loss of generality, a fitting curve in the form $f(\mathbf{x}, C) = \sqrt{c_0 + c^T\mathbf{x}}$ is considered. The choice has been selected for similarities with similar ENTSO-E approaches adopted for the empirical estimation of the aFRR needs for Europe [13,15], supported by numerical evidence of the authors. More details are reported in Appendix B.

4.2. Definition of combinations of system states

To successfully calibrate the non-linear model, the set Ω_X of operational system states need to be defined. This section describes the proposed procedure to populate the set.

First, we define the set of variables that affect the reserve and shall be tracked. Reserve requirements depend on two types of variables in the MILP energy planning problem: (1) planning variables, which remain constant across all time steps of the MILP optimization (e.g., the optimal nominal dimensions for different generators or storage units) and affect reserve requirements due to tripping events, and (2) operational variables or constraints (e.g., the power supplied by vRES technologies, and the loads), which vary throughout the year and impact reserve requests in terms of forecasting uncertainties and VRD.

The following procedure is implemented to manage this process:

1. define the domain in terms of maximum capacities for the variables of the problem (refer to Table A.4 for details);
2. define intermediate values for each dimension; in this study, a uniform discretization of the range of capacities is proposed. For example, let us assume to discretize 10 coal unit plants 400 MW each into 5 steps, each step is separated by 800 MW;
3. generate a sufficiently large set of possible combinations of these values by enumerating the options;
4. simulate these combinations to populate the sample used to fit the non-linear functions necessary for estimating reserve requirements.

The problem size can be increased by: (1) increasing the morphological complexity of the power system (e.g. increasing the number of nodes); (2) increasing the number of components considered in the Monte Carlo simulations; and (3) introducing new types of components. While the first two options have a relatively small impact on the choice of combinations and the runtime required to calibrate the coefficients of the nonlinear function, the third option can increase the computational burden. Expanding the types of components introduces higher dimensional parameter spaces into the Monte Carlo simulations, requiring additional sampling to ensure adequate representation of the expanded parameter space. This in turn increases the computational complexity of the calibration phase. Therefore, the choice of combinations must balance two factors: ensuring uniform sampling across the dimensions affecting the Monte Carlo simulations, and maintaining computational feasibility for both the Monte Carlo phase and the subsequent calibration of non-linear parameters.

5. Comprehensive MILP planning with reserve

The power system planning proposed in this study is based on a MILP problem developed within the PyPSA's framework [25] and properly adapted to account for the proposed reserve modelling discussed above. In the following, the objective function is detailed, the main system constraints and also the reserve modelling, also accounting for

the proposed stochastic reserve model, and its parametrization with non-linear function.

5.1. Objective function

The objective of the problem is minimizing the Total Annualized Costs f_{obj}^{base} of the power system, as outlined in Eqs. (17)–(19). The objective hence accounts for capital costs (CC_{tot}) and the operational costs (OC_{tot}); $w(t)$ denotes the weigh of each time step t into the objective function.

$$\min f_{obj}^{base} = CC_{tot} + OC_{tot} \tag{17}$$

$$CC_{tot} = \sum_{n\in\Omega_N}\left[\sum_{a\in\Omega_G\cup\Omega_R\cup\Omega_S} cc_{a,n}\cdot P_{a,n} + \sum_{s=1}^{\Omega_S} cc_{s,n}\cdot E_{s,n}\right] \tag{18}$$

$$OC_{tot} = \sum_{t\in\Omega_T} w_t\cdot\left(\sum_{n\in\Omega_N}\sum_{a\in\Omega_G\cup\Omega_S} oc_{a,n}\cdot d_{a,n,t}\right) \tag{19}$$

5.2. Main planning constraints

The electrical balance at each of the nth nodes in Ω_N is ensured by Eq. (20), where $f_{ln,t}$ is the power flow in the line lnth with networks' incident matrix $K_{ln,n}$. Eqs. (21)–(23) guarantee that the power generated by the generators and storage power converters, as well as the energy stored in accumulators, always remains within maximum capacity and technical minimum limits, also considering the possibility for components to be turned off through the status variable $s_{a,t}$. Finally, Eq. (24) ensures the balance for each storage unit across different time steps, including the self-discharge coefficient $\eta_{sd,s}$.

$$\sum_{a\in(\Omega_G\cup\Omega_R)} d_{a,n,t} + \sum_{s\in\Omega_R} d_{s,n,t}^{dsc}\cdot\eta_{s,n}^{dsc} + \sum_{ln\in\Omega_{LN}} f_{ln,t}\cdot K_{ln,n} = \sum_{s\in\Omega_R}\frac{d_{s,n,t}^{ch}}{\eta_{s,n}^{ch}} + \sum_{l\in\Omega_L} l_{l,n,t} \tag{20}$$

$$s_{a,n,t}\cdot P_{a,n}\cdot p_{a,n,t}^{min} \le d_{a,n,t} \le s_{a,n,t}\cdot P_{a,n}\cdot p_{a,n,t}^{max}, \quad a\in\Omega_G\cup\Omega_S \tag{21}$$

$$E_{s,n}\cdot e_{s,n,t}^{min} \le e_{s,n,t} \le E_{s,n}\cdot e_{s,n,t}^{max}, \quad s\in\Omega_S \tag{22}$$

$$d_{r,n,t} \le CF_{r,n,t}\cdot P_{r,n}, \quad r\in\Omega_R \tag{23}$$

$$e_{s,n,t} = e_{s,n,t-1}\cdot\eta_{sd,s,n} - d_{s,n,t}^{dsc} + d_{s,n,t}^{ch}, \quad s\in\Omega_S \tag{24}$$

5.3. Reserve requirements

Eq. (27) ensures that the total reserve provided by both generators and storage systems meets the required reserve levels for each type of reserve $\Omega_{R_{rq}}$, as defined by Eq. (26), at any given time step t. Eq. (25) clarifies how, once in the MILP energy planning problem, the $\mathbf{x}$ combinations through which the non-linear functions (R_{rq}^{ToR}) must be entered are uniquely determined per each time step t using, formally, the formulation described in Section 3, or the efficient reformulations described in Section 5.7. The contribution by the assets is modelled in the following subsections.

$$\mathbf{x_t} = (P_a, \dots, CF_{r,t}, \dots, L_t, \dots, VRD_t) \tag{25}$$

$$\Omega_{R_{rq}} = \{\text{FCR, aFRR, mFRR, RR}\} \tag{26}$$

$$\sum_{n\in\Omega_N}\sum_{a\in\Omega_G\cup\Omega_S} r_{a,n,t}^{ToR} \ge R_{rq}^{ToR}(\mathbf{x_t}), \quad \forall\ \text{ToR}\in\Omega_{R_{rq}} \tag{27}$$

It is worth noting that constraint (27), in general, represents a non-linear function that makes the problem non-linear with no general convergence proof [26]. When the constraint (27) defines a convex set, the resulting problem is convex and has been proven to converge to the global optimum with an appropriate solver [26]. However, this is not generally the case, as discussed in Section 4. For this reason, a linearization approach is proposed in Section 5.7.

5.4. Reserve provision by DGs

Eqs. (28)–(30) model the participation of generators in providing reserve supply, per each node in Ω_N. The parameter t_{RR} represents the duration for which RR must be guaranteed, typically up to 2–3 h [13]. For reserve types other than RR, it is unnecessary to consider steps prior to the tth time step, as the standard requires generation of power for a maximum period shorter than 1 h. Eq. (29) limits the total reserve that can be supplied by each generator based on the available but unused power at each time step. Eq. (30) further constrains the power that can be supplied for each type of reserve in $\Omega_{R_{rq}}$ due to the ramp-up capacity specific to each type of generator. The coefficients μ_g^{ToR} are percentage values that limit the power available for allocation to each type of power reserve, specific to each type of generator. This allows for a more accurate representation of the behaviour of different generators, such as the combined-cycle gas turbine, which is less reactive compared to other types of DGs.

$$r_{g,n,t}^{FCR} + r_{g,n,t}^{aFRR} + r_{g,n,t}^{mFRR} + \sum_{i=0}^{t_{RR}} r_{g,n,t-i}^{RR} \le r_{g,n,t}, \quad \forall g\in\Omega_G \tag{28}$$

$$r_{g,n,t} \le P_{g,n}\cdot s_{g,n,t} - d_{g,n,t}, \quad \forall g\in\Omega_G \tag{29}$$

$$r_{g,n,t}^{ToR} \le P_{g,n}\cdot s_{g,n,t}\cdot\mu_{g,n}^{ToR}, \quad \forall ToR\in\Omega_{R_{rq}},\ g\in\Omega_G \tag{30}$$

5.5. Reserve provision by storage systems

Similarly to the case of generators, per each node in Ω_N, Eqs. (31)–(36) model the ability of storage systems to contribute to power reserves. The main difference with the previous formulation is in Eq. (32), which ensures that the sth storage system can provide reserves not only in terms of power that can be provided at time t, but also in terms of energy. This guarantees that once the system has allocated reserve availability to the storage system, it will have enough energy to meet demand for the remaining $t_{RR} - 1$ time steps. Finally, Eqs. (35)–(36) ensure that the ramp-up capacity for different reserves is respected, considering both power conversion and energy nominal capacities.

$$r_{s,n,t}^{FCR} + r_{s,n,t}^{aFRR} + r_{s,n,t}^{mFRR} + \sum_{i=0}^{t_{RR}} r_{s,n,t-i}^{RR} \le r_{s,n,t}, \quad \forall s\in\Omega_S \tag{31}$$

$$r_{s,n,t}^{FCR} + r_{s,n,t}^{aFRR} + r_{s,n,t}^{mFRR} + r_{s,n,t}^{RR} + \sum_{i=1}^{t_{RR}} r_{s,n,t-1}^{RR}\cdot(i+1) \le \eta_{s,n}^{disch}\cdot(e_{s,n,t} - E_{s,n}\cdot e_{s,n,t}^{min}), \quad \forall s\in\Omega_S \tag{32}$$

$$r_{s,n,t} \le \eta_{s,n}^{disch}\cdot(P_{s,n} - d_{s,n,t}), \quad \forall s\in\Omega_S \tag{33}$$

$$r_{s,n,t} \le \eta_{s,n}^{disch}\cdot(e_{s,n,t} - E_{s,n}\cdot e_{s,n,t}^{min}), \quad \forall s\in\Omega_S \tag{34}$$

$$r_{s,n,t}^{ToR} \le P_{s,n}\cdot s_{s,n,t}\cdot\mu_{s,n}^{ToR}, \quad \forall ToR\in\Omega_{R_{rq}},\ s\in\Omega_S \tag{35}$$

$$r_{s,n,t}^{ToR} \le E_{s,n}\cdot s_{s,n,t}\cdot\mu_{s,n}^{ToR}, \quad \forall ToR\in\Omega_{R_{rq}},\ s\in\Omega_S \tag{36}$$

5.6. Definition of variation of residual demand

The variation of the residual demand, once in the MILP energy planning problem, varies for the different t time steps in Ω_T, as represented by Eqs. (37)–(38). VRD_t is the value used to estimate the time series of the reserve requirement, related to the contribution of ramp dynamics.

$$RD_t = \sum_{n\in\Omega_N}\left[\sum_{l\in\Omega_L} l_{l,n,t} - \sum_{r\in\Omega_R} P_{r,n}\cdot CF_{r,n,t}\right] \tag{37}$$

$$VRD_t = RD_t - RD_{t-1} \tag{38}$$

5.7. Linearization approach of reserve parametrization

Although approximations detailed in Section 4 reduces the complexity, the model is still non-linear that makes it difficult to integrate into the MILP optimization framework. For this reason, as widely adopted in the literature [27,28], the non-linear constraint (27) is linearized using a first-order Taylor approximation. This ensures convergence of each iteration conversely to the non-linear formulation. The Taylor expansion denoted in (39) allows reformulating the non-linear constraint (27) into Eq. (40), which ensures convergence of the MILP iteration.

$$f(\mathbf{x}, C) \approx f(\mathbf{x^0}, C) + \sum_i \frac{\partial f}{\partial x_i}(x_i - x_i^0) = k_0 + \sum_i \frac{\partial f}{\partial x_i} x_i = k_0 + \mathbf{k_1^T x} = T_f(\mathbf{x}) \tag{39}$$

$$\sum_{n \in \Omega_N} \sum_{a \in \Omega_G \cup \Omega_S} r_{a,n,t}^{ToR} \geq R_{rq}^{ToR}(\mathbf{x_t}) \approx T_{R_{rq}^{ToR}}(\mathbf{x_t}), \quad \forall \text{ToR} \in \Omega_{R_{rq}} \tag{40}$$

It is worth noticing that as the only non-linearity lies in constraint (27), the proposed procedure allows an efficient decomposition of the complexity of both the reserve and planning models, as denoted in Fig. 1. Specifically, the complex reserve model is efficiently captured using a non-linear formulation and, on the other hand, the iterative convexification (or linearization) is applied to allow its coupling with the MILP planning, similarly to other studies in different contexts [27,28].

5.8. Convergence criterion for MILP planning

As outlined in the previous section, the Taylor approximation is used to linearize the non-linear reserve requirements around each $\mathbf{x_t}$. Iterative adjustments between the MILP planning problem and the Taylor approximations are essential, as depicted in Fig. 2. To determine the stopping criterion, two metrics shall be satisfied for an acceptable number (E.g. 2) of consecutive iterations: (1) the variation of the MILP's objective function cost must be within the tolerance of the optimization solver (Eq. (41)), and (2) the Root Mean Square Error (RMSE) of the results of subsequent iterations of the method must be within tolerance (e.g. 10 MW) (Eqs. (42)–(43)).

$$\frac{|f_{obj,i}^{base} - f_{obj,i-1}^{base}|}{f_{obj,i}^{base}} \leq MIPgap \tag{41}$$

$$\bar{R}_{rq,i}^{ToR} = \sum_{t \in \Omega_T} \frac{\frac{\sqrt{(R_{rq,t,i}^{ToR})^2 - (R_{rq,t,i-1}^{ToR})^2}}{(R_{rq,t,i}^{ToR})}}{T} \tag{42}$$

$$\frac{\sum_{ToR \in \Omega_{ToR}} \frac{\bar{R}_{rq,i}^{ToR}}{4} - \sum_{ToR \in \Omega_{ToR}} \frac{\bar{R}_{rq,i-1}^{ToR}}{4}}{\sum_{ToR \in \Omega_{ToR}} \frac{\bar{R}_{rq,i}^{ToR}}{4}} \leq 10 \quad MW \tag{43}$$

This criterion ensures that the planning iterations progress towards a stable solution, minimizing cost and aligning closely with actual reserve needs.

6. Case study: the South African power system

6.1. Description

In this study we validate and apply the proposed methodology for the optimal capacity expansion planning of South Africa in 2050. This case study is deemed particularly meaningful because of the country's RES potential and the ongoing challenges in terms of generation adequacy that is leading to significant load shedding. Moreover, it proves as validation for a methodology typically implied only for European countries and here extended to global scope.

Table 1
Comparison of the non-linear functions approx. with nowadays Eskom requests.

Type of reserve	Reserve requests (MW)	
	Non-linear functions (min – max)	Eskom (min – max)
FCR	1125 (1120–1225)	1195–1395
aFRR	206 (155–422)	

Table 2
Comparison of the non-linear functions approx. with stochastic reserve estimations.

Type of reserve	MAE	RMSE
FCR	12.6 MW	19.5 MW
aFRR	1.0 MW	5.9 MW
mFRR	3.3 MW	7.2 MW
RR	3.4 MW	6.5 MW

It should be noted that South Africa represents a net energy exporter in the region and imports from neighbouring countries represents less than 4% of the total annual electricity supply in South Africa [29]. By considering also the scope of the paper, the role of the interconnection in the system stability has been kept for future studies.

6.2. Scenarios definition

As least-cost planning for South Africa 2050 is proposed, corresponding estimates for costs, technology availability, and demand are considered. Actual system data is also used to validate marginal cost assumptions. For 2050, two scenarios are considered:

- 2050-Cost Efficient (CE2050) scenario. There are no constraints on the type of plant planned, and the only objective is to minimize the NPC (see Section 5), and a carbon tax on emissions from coal, gas and diesel power stations is considered;
- 2050-Fully Decarbonized (FD2050) scenario: only renewable technologies and storage are considered, assuming the development of RES control systems that assimilate the inertia reserve requirements to the FCR problem.

Due to computational limitation, we employ 42 typical days with hourly electrical balancing and a 10-nodes system representation, consistent with other studies for the country [30]. This approach balances the need for capturing seasonal and diurnal variations with the importance of maintaining geographic differentiation across nodes. Existing power plants and the technical potential for installations in 2050 are reported in A.4.

Hourly load profiles are provided by Eskom [29] (the local system operator) while the nodal capacity factor curves for solar PV and wind across the different regions are obtained from the ERA5 web platform [31]. The total technical potential for all vRES technologies, dispatchable generation, and pumped hydro storage is distributed among the 10 nodes based on literature information. Li-ion battery energy storage system (Li-ion) and hydrogen storage (H2) are assumed to be equally available across the nodes. According to *The Carbon Tax Act*, a carbon tax of $100/tonne of equivalent gas emissions is applied to diesel, gas, and coal power plants [32]. A.6 shows the assumed percentage contribution to reserve by different technologies, and A.7 lists the storage technology parameters.

6.3. Reserve parameters

To successfully calibrate the reserve parameters of the methodology described in Section 2, we collected the installed capacities of the power plants, their expected yearly failures and estimates of forecasting uncertainties. Then, the set E of combinations is defined to train the calibration model as denoted in Section 4. In particular, to dominate

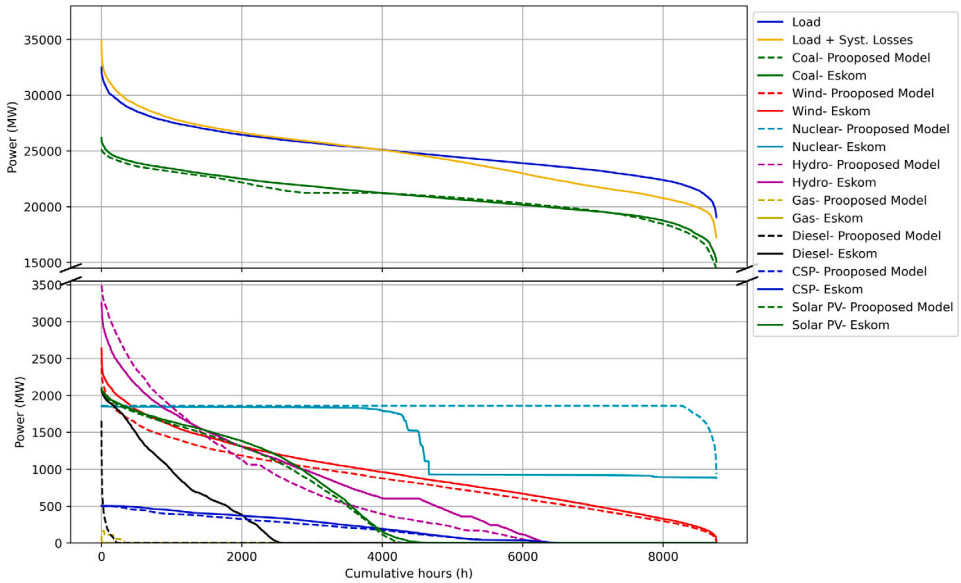

Fig. 4. Graphical comparison between the power supplied by the different plants in the dispatch strategy recorded by Eskom and the value obtained by optimizing the MILP energy problem (without planning variables).

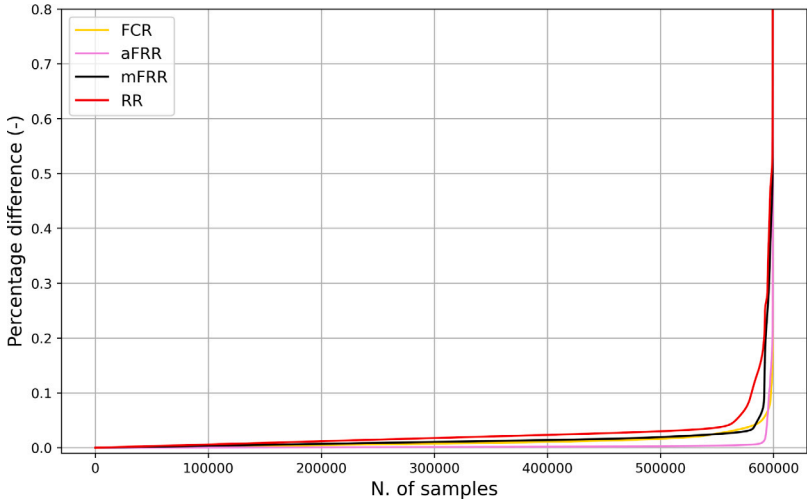

Fig. 5. Percentage difference between reserve reqs. estimated with stochastic model and the fitted non-linear functions.

the numberosity, existing power plant units are grouped by size, type, and failures per year (λ_a), as shown in A.4. The table also reports that the current maximum load is 35.6 GW, while in 2050, the growth in electrical demand will increase it to 60.5 GW with a maximum VRD of ±3 GW. For vRES generation and load, the standard deviation related to the forecasting error is estimated in agreement to the literature and measurements obtained by Eskom [29]. Capital, maintenance, and marginal costs are detailed in A.5, highlighting the differences between current costs and those projected for 2050, where a reduction is expected.

For simplicity, the installed coal-fired plants are set to produce at least 30% of their nominal power for each time of the simulated MILP problem, which is deemed realistic as these power plants do have the lowest marginal cost in South Africa and thus, if available, it is likely they operate for base load. Moreover, the contribution of the diesel and gas plants to the primary reserve is considered null (as shown in Table A.6). This last assumption is based on the following consideration: diesel and gas plants can only provide reserve when they are running, and in the actual South African system, also due to the high marginal costs, they are actually running only in a limited number of cases (under peak load conditions). By setting their contribution to the primary reserve to zero, the optimization will eventually lead to them not being selected or contributing to the power reserve, but primarily to respond to peak load needs. Finally, this set of assumptions, based on the analysis of the operating state of the current system, is further analysed in Section 6.4.

6.4. Validation of the assumptions

To validate the cost assumptions reported in Table A.5 and the application of the model for reserve estimation, a MILP dispatch optimization is executed with no capacity expansion, hence considering only the existing power plants. Specifically, the MILP problem described in Section 5 is run without including reserve requirements and without optimizing the nominal capacity, as the actual capacities are treated as fixed. The objectives of this optimization is: (1) understand how the model schedules the production from different power plants; (2) estimate the reserve required for the optimized schedule through

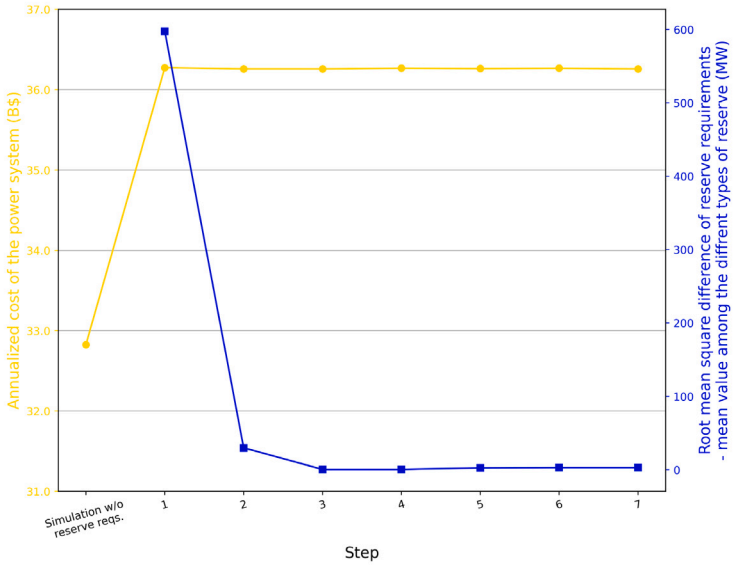

(a) CE2050

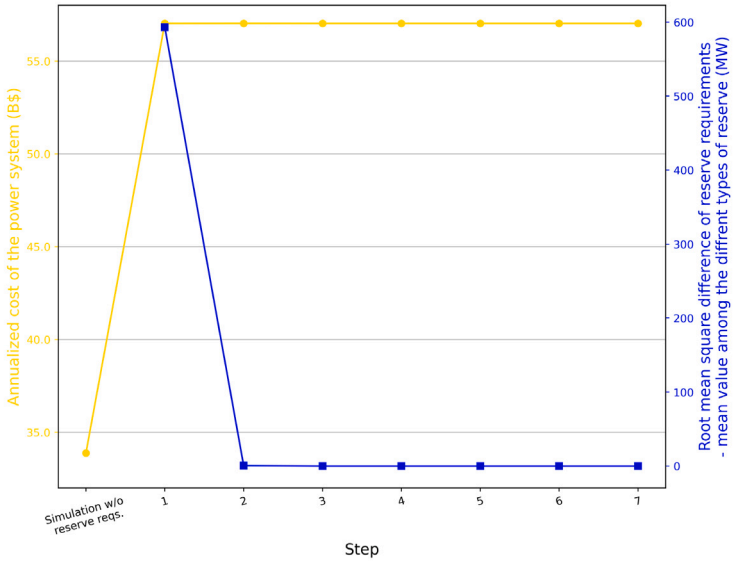

(b) FD2050

Fig. 6. Convergence of iterations.

post-processing; (3) compare the results with actual data collected from Eskom.

Fig. 4 shows the mean hourly power supplied from different resources over the year, comparing the optimized values from the MILP energy model with the recorded data from Eskom [29]. The MILP problem, excluding planning variables, is run to meet nodal load profiles (denoted as "Load" in the plot), corresponding to the annual residual demand, excluding system losses, manual load reductions, and negligible production from other RES tecs not implemented in the model. Coal power plants are constrained to operate at a maximum capacity of 75% of their nominal capacity and an annual average power output of 60% of nominal capacity to reflect typical outages managed by Eskom. The results demonstrate that the assumed costs replicate scheduling decisions close to actual operations, with coal plants supplying power above 30% of nominal capacity, justifying a minimum operating power percentage in the MILP model. Small discrepancies in nuclear generation profiles are attributable to planned and unplanned full or partial outages reflected in Eskom's data. In contrast, the MILP energy planning optimization accounts for potential outages through reserve requirements, yet it schedules units under the assumption of their full availability. The limited role of diesel and gas plants during peak hours supports excluding their contribution to FCR and aFRR.

Lastly, the non-linear function parameters for the reserve estimation, presented in the following Section, is applied to compare the reserve requirements estimated by the proposed non-linear model with

Table 3
Optimal nominal power identified for the 2 scenarios 2050.

	CE2050 (GW)		FD2050 (GW)	
Reserve Reqs.	No	Yes	No	Yes
Iteration	0	7	0	7
Coal	0	19.5	–	–
Nuclear	1.9	1.9	1.9	1.9
Diesel	3.1	3.1	–	–
Gas	0.8	0.8	–	–
HP	0	0	0	0.6
PHS	11.4	11.4	11.4	11.4
CSP	0	0	6.8	10.0
PV	80.5	64.9	80..5	80.5
WT	118.9	90.8	125.0	125.0
Li-ion	13.4	24.2	16.5	51.3
H2	24.7	7.6	23.9	156.7

the actual values used by Eskom. Table 1 shows that the proposed model aligns well with Eskom's reserve requests, with acceptable differences.

7. Results and discussion

7.1. Estimation of reserve requirements

According to Section 3, to successfully calibrate the non-linear parametric function ($f(x, C) = \sqrt{c_0 + c^T \mathbf{x}}$), the stochastic reserve model is used to map a sufficiently large number of combinations that define the possible operating region of the future energy system. This phase represents the most computationally demanding step, with simulation times ranging from 10 to 60 s per combination (with 10 processes in parallel), totalling approximately 320 h. In agreement to Section 4.2, the combinations are drawn using the maximum capacity of resources shown in Table A.4 for a total of about 600,000 combinations. The coefficients of the non-linear function are calibrated using the results derived from the Monte Carlo simulations. The outcomes of this fitting procedure are presented in Fig. 5 and Table 2.

The curves in Fig. 5 show the absolute normalized difference between the reserve estimated with the fitted coefficients and the reserve requirements obtained with the stochastic model. Table 2 reports the values assumed by the most meaningful metrics of model prediction accuracy, in terms of the comparison between the non-linear fit and the values obtained in the output from the stochastic reserve model. The results indicate that the assumed coefficients and the shape of the function provide a good fit to the reserve estimates across the different combinations, ensuring minimal loss of accuracy during the transition from the full stochastic reserve model to its non-linear parametrization. Details on the explicit fitting curve and the optimal parameters are shown in Appendix B.

7.2. Optimized CE2050 and FD2050 scenarios

The MILP optimization process is evaluated for two scenarios: CE2050 and FD2050. Fig. 6 shows the convergence of the iterations for both scenarios. The results show effective convergence within four iterations, ensuring reliable solutions. Each optimization of the MILP energy planning problem with reserve requirements required a computational time ranging from 1 to 10 h per iteration, with an average runtime of approximately 5 h. These times highlight the computational complexity of integrating reserve requirements into the planning model and the iterative process necessary to achieve convergence. However, to ensure the convergence of the algorithm, up to eight optimization have been performed. The results of the 8th iteration are selected as the final results of the MILP energy planning problem, and the optimal solution for CE2050 corresponds to an total annual cost of B$36, while the for FD2050 corresponds to B$57. Results are also validated

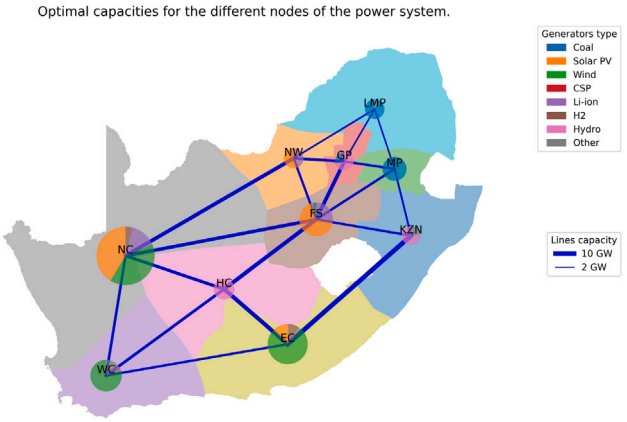

(a) CE2050

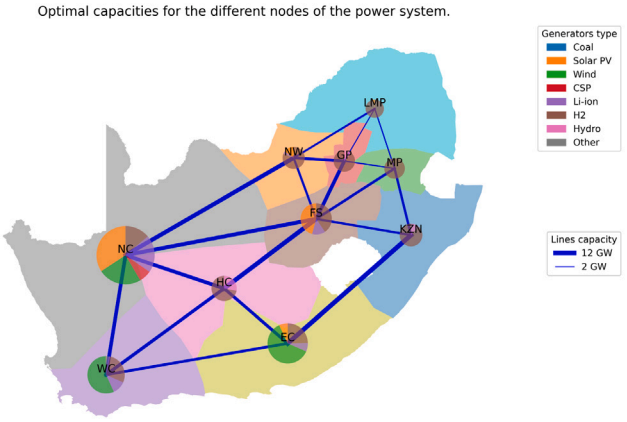

(b) FD2050

Fig. 7. Optimal configuration of the system among the different nodes.

with respect to a similar planning study by Meridian Economics [33], whose comparison is reported in Appendix C that further confirms the robustness of the model.

Table 3 summarizes the optimal nominal power capacities identified for the two scenarios and compares them with the results obtained from iterations without reserve requirements integrated into the MILP energy planning model. The CE2050 scenario includes a mix of coal, nuclear and renewables, while the FD2050 scenario focuses exclusively on renewables and storage technologies. In FD2050, the absence of fuel-fired plants leads to the saturation of HP and CSP, which are not selected in CE2050. PV and wind turbines (WTs) are also saturated in FD2050, with an increase of 24% and 38% in the optimal nominal power compared to the CE2050 scenarios. Pumped-Hydro Storage (PHS) is saturated in both scenarios, but the BESS and H2 show a steady increase in installed power due to the need to support the increase in vRES generation tecs. Due to technical potential constraints, installed WTs increase more than PV, and this leads to favour H2 (which is seasonal storage), whose optimal nominal power is increased by about 20 times. Fig. 7 shows the optimal configuration of the system between different nodes, illustrating the spatial distribution of capacities for both scenarios and the optimal capacity identified for the transmission system among nodes.

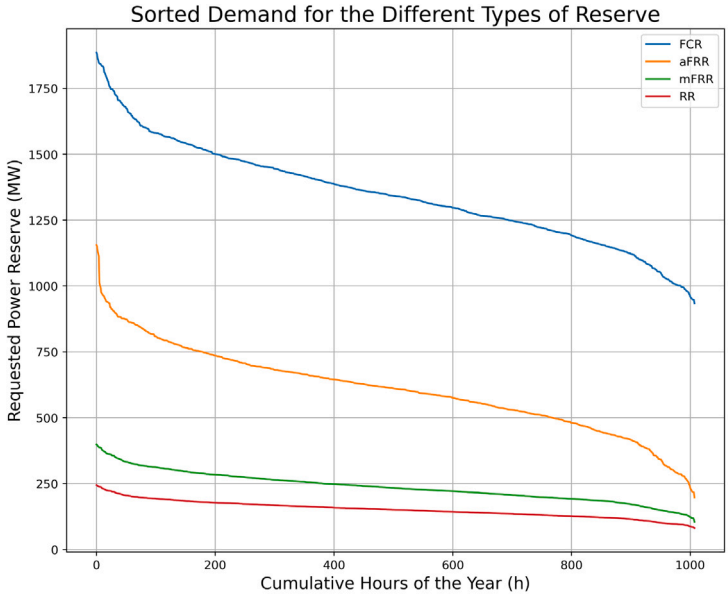

(a) CE2050

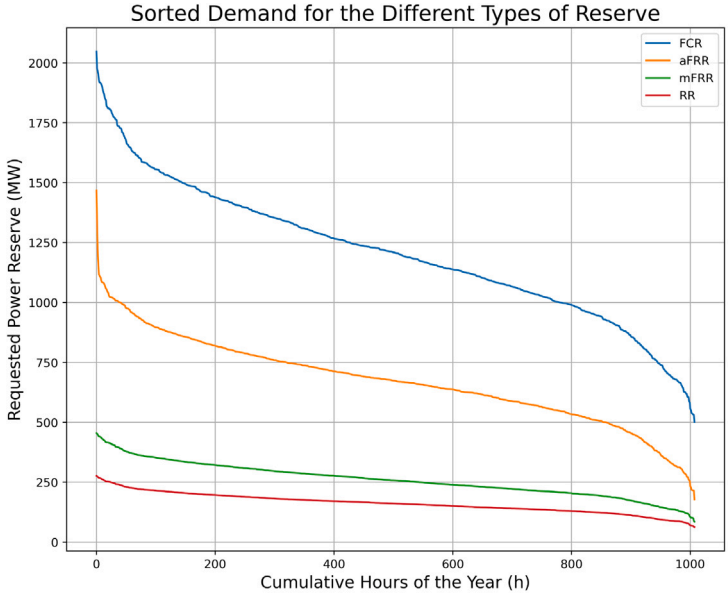

(b) FD2050

Fig. 8. Annual reserve requests sorted in descending order.

Fig. 8 compares the annual reserve requirements for CE2050 and FD2050. The curves show that the FRR requirement is comparable to the FCR, indicating that the reserve requirements are similar despite the significant differences in technology settings. The increase in all types of reserves compared to the current system is consistent across both scenarios. However, the FD2050 scenario exhibits peaks in FCR and aFRR requests that are 10%–15% higher than those in the CE2050 scenario. These higher requests are limited to a few simulated hours, beyond which the reserve requirements in both scenarios are comparable when sorted by hours. Fig. 9 shows how the different technologies contribute to the supply of the different types of reserves. PHS contributes to satisfy the reserve requirements in both the scenarios. However, in CE2050 PHS alone fully satisfies the demand, whereas in FD2050 most of the demand is met by Fuel-Cell (FC). The choice of these two types of technologies to satisfy the reserve is due to the seasonal behaviour of these two types of storage: their low discharge efficiency compared to Li-ion BESS means that they are almost fully charged for almost all simulated snapshots, allowing them to respond more effectively to flexibility requirements and better than other types of generation components, which on the contrary are most dedicated to providing electricity. In FD2050, H2 is preferred to PHS for reserve requirements due to the lower capital cost of the storage components, its higher maximum capacity and the preference of the system to use PHS for operational purposes (with higher round-trip efficiency compared to the H2 cycle).

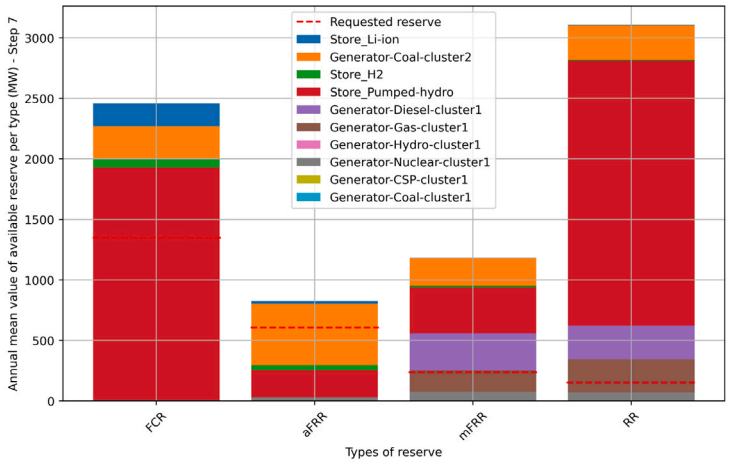

(a) CE2050

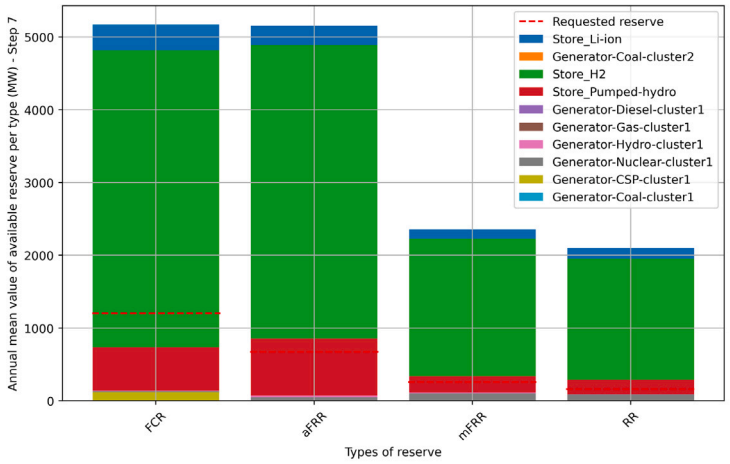

(b) FD2050

Fig. 9. Reserve allocation among the different tecs.

The MILP optimization results highlight the benefits of incorporating storage and renewable energy technologies to meet future energy demands, as demonstrated in the CE2050 scenario. Specifically, CE2050 shows that BESS and H2 can significantly contribute to the supply of all types of reserves in a cost-efficient manner, even outperforming currently used gas emission technologies. Additionally, this scenario illustrates how vRES can be cost-efficient for power supply, despite leading to higher reserve requests due to uncertainties in their variability. The FD2050 scenario, on the other hand, reveals the costs associated with full decarbonization, highlighting that a 100% RES solution is not yet fully economically competitive, with a 56% higher total annualized cost compared to CE2050. However, the FD2050 scenario also demonstrates the consistent role that H2 could play in the final stages of the transition, suggesting a more significant role for seasonal storage in achieving a fully renewable energy system.

7.3. The role of reserve requirements

Table 3 clearly highlights the role of integrating reserves requirements estimation into the MILP energy planning problem. In CE2050, the MILP initially prefers RES capacity over coal plants. However, when reserve requirements are integrated (iteration 7), the model increases the utilization of coal plants to ensure adequate reserve, while reducing WT capacity by 25% and PV capacity by 20% due to the unpredictability of RES. The increased need for flexibility also leads to a significant 85% increase in BESS capacity, despite the reduction in RES. Conversely, H2 capacity decreases due to its dependence on WT. In the FD2050 scenario, the need for increased flexibility in a 100% RES system is met by an increase in electricity generation capacity. In fact, CSP increases from 6.8 GW to 10 GW, as PV and WT have already reached their technical potential limits in the no-reserve-requirement scenario. This scenario further underlines the critical importance of storage technologies to ensure system flexibility, as BESS and H2 capacities increase by a factor of 2.1 and 5.6 respectively.

8. Conclusions

This paper presents an integrated approach for energy system planning that incorporates a stochastic model for reserve estimation suitable for future energy scenarios with high penetration of variable renewable

energy sources. By combining a stochastic reserve estimation approach with an iterative MILP energy planning model, this work successfully provides a robust framework, ensuring system stability, and guiding strategic decisions for a sustainable energy transition.

The applicability of the proposed methodology is demonstrated through the case study of South African power system, highlighting its relevance for the type of challenges it is currently facing. Extensive validation of the methodology is performed using actual data from the South African Transmission System Operator Eskom.

The validation proves the stochastic methodology based on Monte Carlo scenario for estimating reserve requirements is able to capture existing values for the South African system adopted by Eskom.

The integration of the stochastic reserve estimation model into the MILP energy planning framework reveals its significant impact on optimizing the energy mix. In the cost-efficient scenario (CE2050), where the only objective is to minimize the NPC without constraints on the type of plant planned, incorporating reserve requirements shifts the preference from higher WT and PV capacities to a more balanced inclusion of coal plants, reducing WT and PV capacities by 25% and 20%, respectively. Additionally, the model highlights that energy storage techs are essential for meeting flexibility demand and their cost effectiveness. This shift demonstrates the model's ability to adapt the energy system configuration to ensure both cost-effectiveness and system reliability. In contrast, the 100% RES scenario (FD2050) reveals the economic challenges of full decarbonization, with total annualized costs 56% higher than in the cost-efficient scenario. Despite this, the 100% RES scenario also highlights the critical role that H2 storage is likely to play in the eventual transition to a fully renewable energy system (also linked to the increase in installed WT in 100% RES compared to the cost-efficient scenario), highlighting the importance of seasonal storage solutions in a decarbonized future.

In summary, this study demonstrates the effectiveness of an integrated stochastic approach for reserve estimation to energy planning, providing a robust framework for addressing the complexities of modern power systems and supporting the transition to a low-carbon energy future.

CRediT authorship contribution statement

Enrico Giglio: Writing – original draft, Software, Methodology, Conceptualization. **Davide Fioriti:** Writing – original draft, Supervision, Methodology, Conceptualization. **Munyaradzi Justice Chihota:** Writing – review & editing, Data curation. **Davide Poli:** Writing – review & editing. **Bernard Bekker:** Writing – review & editing, Resources. **Giuliana Mattiazzo:** Writing – review & editing, Resources.

Declaration of competing interest

The authors declare that they have no known competing financial interests or personal relationships that could have appeared to influence the work reported in this paper.

Acknowledgements

This work was partially supported by the Italian Ministry of University and Research (MUR) CUP I53C23002650007 (RESILIENT) within the CETPartnership Joint Call 2022 (https://cetpartnership.eu/). As such, it has also received funding from the European Union's Horizon Europe research and innovation programme under grant agreement no. 101069750.

This research was supported by the National Research Foundation of South Africa (Grant Number: 150529).

This work was supported by the Politecnico di Torino through the CRUI CARE Agreement.

Table A.4
Main parameters assumed for the definition of the case study.

Cluster	P_{nom} (MW)	n_{mod}^{act}	$n_{mod,max}^{2050}$	λ (trips/yr)	σ (%)	Refs.
Coal-1	590	48	48	42.5	–	[34]
Coal-2	195	40	40	42.5	–	[34]
Nuclear	930	2	2	1.68	–	[34]
Diesel	155	20	20	12.2	–	[34]
Gas	55	14	14	12.2	–	[34]
Hydro-1	70	9	9	4.9	–	[34]
PHS	265	11	43	4.9	–	[34]
CSP	100	5	100	15.8	–	[34]
PV	100	24	805	0.4	15.0%	[35,36]
WT	100	32	1500	2.5	17.6%	[37,38]
Li-ion	100	–	10 000	0.8	–	[39]
H2	100	–	2000	3.5	–	[40]
Load-act-max	35 600	–	–	–	3.5%	[29]
Load-2050-max	60 500	–	–	–	3.5%	[41]
VRS	±3000	–	–	–	–	

Appendix A. Summary of assumed values.

See Table A.4–A.7.

Appendix B. Coefficients of non-linear functions for estimating reserve reqs

As described in Section 4, we considered a non-linear function in the form $f(\mathbf{x}, C) = \sqrt{c_0 + c^T \mathbf{x}}$ whose explicit form for the mathematical problem shown in Section 5 is detailed in Eq. (B.1) for each of the four types of reserve (ToR). The coefficients of the equation calibrated for the South African case study detailed in Section 7.1 are then detailed in Table B.8.

$$R_{rq}^{ToR}(\mathbf{x_t}) = \left(\sum_{a \in \Omega_G \cup \Omega_S} \alpha_a^{ToR} \cdot P_a \cdot s_{a,t} + \sum_{r \in \Omega_R} \beta_r^{ToR} \cdot P_r \cdot CF_{r,t} + \sum_{l \in \Omega_L} \gamma_l^{ToR} \cdot L_{l,t} + \delta^{ToR} \cdot \sum_{l,r \in \Omega_L, \Omega_R} VRD_t + \varepsilon^{ToR} \right)^{\frac{1}{2}} \tag{B.1}$$

Appendix C. Comparison of CE2050's results with a cost-efficient 2050 South African power system study incorporating reserve requirements from a deterministic model

Optimal energy planning results of CE2050, proposed in Table 3, were also compares with Meridian Economics's study [33], that assessed the unconstrained least-cost (ULC-2050) energy mix for the South African system in 2050. In [33], reserves were considered deterministically by applying a 10% planning reserve margin as a generation capacity headroom with respect to general technology capacity credits. Given such differences in objectives as well as other input assumptions, direct comparison of the two models may not be fully feasible. Nevertheless, this comparison can provide valuable insights and reveal critical convergences and divergences in energy planning strategies.

The comparison of the scenarios is shown in Fig. C.10 and the results indicate that both of them allocate comparable capacities to Solar PV and WT. This alignment highlights the similarities in the core cost optimization attributes of both models. In both models, the optimum solution does not utilize CSP, favouring Solar PV supported by other storage technologies. The solutions in both models are resolute on nuclear, as they saturate the existing installed capacity.

A notable divergence in the usage of coal are attributed to assumptions on the decommissioning of coal in the future. The ULC-2050 applies decommissioning rates aligned to the 2019 IRP. In contrast, the CE2050 assumes no decommissioning, as supported by historical delays in decommissioning schedules and the uncertainties over decisions or

Table A.5
Costs assumed for the different network components. *Stack lifetime of 10 years, with 50% stack [42].

Type of technology	Ref. cost	Life (yr)	CapEx	Degr. Cost	Fixed OpEx	Marg. Cost	Refs.
Coal-1	act.	50	2.8 $\frac{M\$}{MW}$	3.6 $\frac{\$}{MWh}$	70 $\frac{k\$}{MW\ y}$	26.4 $\frac{\$}{MWh}$	[30,43]
Coal-2	act.	50	2.8 $\frac{M\$}{MW}$	4.2 $\frac{\$}{MWh}$	70 $\frac{k\$}{MW\ y}$	31.8 $\frac{\$}{MWh}$	[30,43]
Nuclear	act.	60	6.0 $\frac{M\$}{MW}$	3.3 $\frac{\$}{MWh}$	45 $\frac{k\$}{MW\ y}$	5.9 $\frac{\$}{MWh}$	[30,43]
Diesel	act.	30	0.9 $\frac{\$}{MW}$	5 $\frac{\$}{MWh}$	7.5 $\frac{k\$}{MW\ y}$	170 $\frac{\$}{MWh}$	[43,44]
Gas	act.	30	0.60 $\frac{M\$}{MW}$	1.4 $\frac{\$}{MWh}$	10.2 $\frac{k\$}{MW\ y}$	120 $\frac{\$}{MWh}$	[43,44]
HP	act.	60	3.7 $\frac{M\$}{MW}$	25 $\frac{\$}{MWh}$	15 $\frac{k\$}{MW\ y}$	–	[30,43]
PHS	act.	50	1.5 $\frac{M\$}{MW}$	25 $\frac{\$}{MWh}$	15 $\frac{k\$}{MW\ y}$	–	[30,43]
CSP	act.	30	4.5 $\frac{M\$}{MW}$	5 $\frac{c\$}{MWh}$	40 $\frac{k\$}{MW\ y}$	–	[30,43]
CSP	2050	30	3.3 $\frac{M\$}{MW}$			–	[30,43]
PV	act.	25	0.9 $\frac{M\$}{MW}$	–	16.4 $\frac{k\$}{MW\ y}$	–	[30,43]
PV	2050	25	0.5 $\frac{M\$}{MW}$	–		–	[30,43]
WT	act.	20	1.3 $\frac{M\$}{MW}$	–	52 $\frac{k\$}{MW\ y}$	–	[30,43]
WT	2050	20	0.9 $\frac{M\$}{MW}$	–		–	[30,43]
Li-ion:Storage	2050	15	0.2 $\frac{M\$}{MWh}$	30 $\frac{\$}{MWh}$	6 $\frac{k\$}{MW\ y}$	–	[43,45]
Li-ion:P.Conv.	2050	20	0.4 $\frac{M\$}{MW}$		12 $\frac{k\$}{MW\ y}$	–	[43,45]
H2:Tank	2050	20	0.01 $\frac{M\$}{MWh}$	–	–	–	[42,45]
H2:FC	2050	20*	0.65 $\frac{M\$}{MW}$	–	19.5 $\frac{k\$}{MW\ y}$	–	[45,46]
H2:PEM	2050	20*	0.80 $\frac{M\$}{MW}$	–	32.0 $\frac{k\$}{MW\ y}$	–	[45,46]
Trans. line	–	40	555 $\frac{\$}{MW\ km}$	–	10 $\frac{\$}{MW\ km\ y}$	–	[47,48]

Table A.6
Percentage contribution of different generation components to different reserve types.

Power reserve supplier	Percentage contribution (w.r.t. P_{mod}) to				Refs.
(P_{mod})	FCR	aFRR	mFRR	RR	
Coal-1 (595 MW)	3%	30%	90%	100%	[49,50]
Coal-2 (195 MW)	3%	30%	90%	100%	[49,50]
Nuclear (930 MW)	1%	4%	10%	10%	[51]
Diesel (155 MW)	0%	0%	100%	100%	[49]
Gas (55 MW)	0%	0%	100%	100%	[49]
HP (70 MW)	25%	100%	100%	100%	[50]
PHS (265 MW)	25%	100%	100%	100%	[50]
CSP (100 MW)	3%	0%	0%	0%	[52]
PV (100 MW)	0%	0%	0%	0%	–
WT (100 MW)	0%	0%	0%	0%	–
Li-ion (100 MW)	100%	100%	100%	100%	[53]
H2 (100 MW)	30%	100%	100%	100%	[54]

Table A.7
Assumption of technical parameters describing the behaviour of storage technologies.

Storage tecs.	Efficiency	Self-discharge	Duration Range (h)	Ref.
Li-ion BESS	Round-trip efficiency 90%, equally divided between charge and discharge	0.1 $\frac{\%}{h}$	0.5–2	[55]
EL	65%	–	1–10	[42,56]
FC	51%	–	1–10	[42,56]
H2 tank	–	0% (negligible)	–	[42]
PHS	Round-trip efficiency 76%, equally divided between charge and discharge	0% (negligible)	60–75	[57,58]

policies concerning plant decommissioning and life extension. Despite the differences in the applied domain, the ULC-2050 seems to favour an enhanced Diesel and Gas plant coupled to Auxiliary Steam Turbine Generators (Aux STG). The CE2050 opts for increased PHS use with 8.5 GW more than the ULC-2050.

The CE2050 model also demonstrates a stronger emphasis on advanced flexibility sources, which is aligned to its objective on optimal reserve allocation. It allocates 24.2 GW to Energy Storage and a further 7.6 GW to Hydrogen (H2), compared to the CE-DRM's 14.7 GW and 0 GW, respectively. This allocation signifies the CE2050's advanced

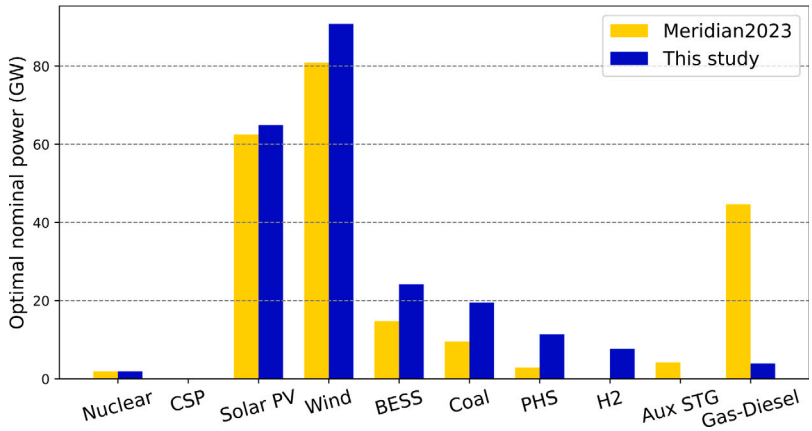

Fig. C.10. Comparison of proposed model's energy planning system results (CE2050) to [33]'s results.

Table B.8
Coefficients of non-linear functions fitted for estimating the reserve requirements, w.r.t. Eq. (B.1). All coefficient are expressed in $\frac{MW^2_{ToR}}{MW_{online}}$.

		FCR	99.7%	99%	95%
Trip. dim.	Coal1	13.40	1.22	0.52	0.12
	Coal2	37.52	3.12	1.78	0.56
	Wind	0.52	0.01	0.01	0.01
	Nuclear	11.17	2.65	0.99	0.00
	Hydro-1	22.38	1.36	0.01	0.01
	PHS	1.70	0.18	0.10	0.02
	Gas	6.94	0.01	0.01	0.01
	Diesel	2.33	0.11	0.05	0.01
	CSP	2.84	0.21	0.12	0.02
	Li-ion	0.15	0.01	0.01	0.00
	H2	0.64	0.04	0.02	0.01
Oper. dim.	PV	0.07	0.01	0.01	0.01
	Wind	23.06	21.31	15.48	7.86
	PV	16.79	15.51	11.25	5.70
	Load	0.85	0.98	0.67	0.29
	VRD	50.34	48.50	40.41	31.14
Fixed (MW^2_{ToR})		0	2.903.88	0	0

approach to incorporating storage technologies, which enhances its ability to manage variability and support grid stability.

Overall, these differences highlight the importance of model assumptions, particularly concerning reserve allocation, in shaping energy planning outcomes, with particular reference to storage technologies (BESS and H2). This analysis highlights the relevance of understanding how various models and the respective assumptions influence the energy model's results.

Data availability

The links to the codes used in this study have been provided in the References.

References

[1] F. Ahmed, D. Al Kez, S. McLoone, R.J. Best, C. Cameron, A. Foley, Dynamic grid stability in low carbon power systems with minimum inertia, Renew. Energy 210 (2023) 486–506, http://dx.doi.org/10.1016/j.renene.2023.03.082, URL https://www.sciencedirect.com/science/article/pii/S0960148123003774.

[2] International Renewable Energy Agency (IRENA), 100% renewable energy scenarios: Supporting ambitious policy targets, 2024, https://www.irena.org/-/media/Files/IRENA/Agency/Publication/2024/Mar/IRENA_Coalition_100_RE_scenarios_2024.pdf.

[3] L. Bongers, N. Mararakanye, B. Bekker, Operating reserve dimensioning methodologies for renewable energy aligned power systems, in: 2021 56th International Universities Power Engineering Conference, UPEC, 2021, pp. 1–6, http://dx.doi.org/10.1109/UPEC50034.2021.9548228.

[4] E. Heylen, F. Teng, G. Strbac, Challenges and opportunities of inertia estimation and forecasting in low-inertia power systems, Renew. Sustain. Energy Rev. 147 (2021) 111176, http://dx.doi.org/10.1016/j.rser.2021.111176, URL https://www.sciencedirect.com/science/article/pii/S1364032121004652.

[5] European Network of Transmission System Operators for Electricity (ENTSO-E), Inertia and rate of change of frequency (rocof), 2020, https://eepublicdownloads.entsoe.eu/clean-documents/SOC%20documents/Inertia%20and%20RoCoF_v17_clean.pdf.

[6] E. Ela, M. Milligan, B. Kirby, Operating Reserves and Variable Generation, NREL/TP-5500-51978; TRN: US201118, http://dx.doi.org/10.2172/1023095, URL https://www.osti.gov/biblio/1023095.

[7] European Network of Transmission System Operators for Electricity (ENTSO-E), All ce tsos' agreement on the methodology to assess the risk and evolution of the risk of exhaustion of fcr in accordance with article 131(2) of the commission regulation (eu) 2017/1485 of 2 august 2017 establishing a guideline on electricity transmission system operation, 2018, https://eepublicdownloads.entsoe.eu/clean-documents/nc-tasks/SOGL/SOGL_A118.1_180808_CE%20SAOA%20part%20B_final_180914.pdf.

[8] M. Caprabianca, M.C. Falvo, L. Papi, L. Promutico, V. Rossetti, F. Quaglia, Replacement reserve for the italian power system and electricity market, Energies 13 (11) (2020) http://dx.doi.org/10.3390/en13112916, URL https://www.mdpi.com/1996-1073/13/11/2916.

[9] International Renewable Energy Agency (IRENA), Innovation landscape brief: Co-operation between transmission and distribution system operators, 2020, URL https://www.irena.org/-/media/Files/IRENA/Agency/Publication/2020/Jul/IRENA_TSO-DSO_co-operation_2020.pdf?la=en&hash=5D78444F4339DC130204A0F9A99A30753368AABC.

[10] D. Ribó-Pérez, L. Larrosa-López, D. Pecondón-Tricas, M. Alcázar-Ortega, A critical review of demand response products as resource for ancillary services: International experience and policy recommendations, Energies 14 (4) (2021) URL https://www.mdpi.com/1996-1073/14/4/846.

[11] Eskom, Ancillary services technical requirements for 2023/24–2027/28, 2022, URL https://www.eskom.co.za/wp-content/uploads/2022/10/240-159838031ASTR2023-2027rev1.pdf. (Accessed 20 June 2024).

[12] European Network of Transmission System Operators for Electricity (ENTSO-E), Explanation of fcr energy requirement for ce and ne as defined in nc lfcr, 2013, https://extranet.acer.europa.eu/Media/Events/Invitation_to_the_expression_of_views_on_the_Network_Code_on_Load-Frequency_Control_and_Reserves/ACERs%20Evaluation/1/2-%20Explanation%20of%20FCR%20Energy%20Requirement%20for%20CE%20and%20NE%20as%20Defined%20in%20NC%20LFCR.pdf.

[13] European Network of Transmission System Operators for Electricity (ENTSO-E), Load-frequency control and performance, 2009, https://www.entsoe.eu/publications/system-operations-reports/operation-handbook/, uCTE OH – Policy 1.

[14] F. Bovera, G. Rancilio, D. Falabretti, M. Merlo, Data-driven evaluation of secondary- and tertiary-reserve needs with high renewables penetration: The italian case, Energies 14 (8) (2021) http://dx.doi.org/10.3390/en14082157, URL https://www.mdpi.com/1996-1073/14/8/2157.

[15] A. van Stiphout, K. De Vos, G. Deconinck, The impact of operating reserves on investment planning of renewable power systems, IEEE Trans. Power Syst. 32 (1) (2017) 378–388, http://dx.doi.org/10.1109/TPWRS.2016.2565058.

[16] T. Brijs, A. van Stiphout, S. Siddiqui, R. Belmans, Evaluating the role of electricity storage by considering short-term operation in long-term planning, Sustain. Energy Grids Netw. 10 (2017) 104–117, http://dx.doi.org/10.1016/j.segan.2017.04.002, URL https://www.sciencedirect.com/science/article/pii/S2352467716301102.

[17] S. Bhavsar, R. Pitchumani, M. Ortega-Vazquez, A reforecasting-based dynamic reserve estimation for variable renewable generation and demand uncertainty, Electr. Power Syst. Res. 211 (2022) 108157, http://dx.doi.org/10.1016/j.epsr.2022.108157, URL https://www.sciencedirect.com/science/article/pii/S037877962200373X.

[18] Terna, [Regulations], 2024, URL https://www.terna.it/en/electric-system/capacity-market/regulations. (Accessed 05 May 2024).

[19] D. Groppi, F. Feijoo, A. Pfeifer, D.A. Garcia, N. Duic, Analyzing the impact of demand response and reserves in islands energy planning, Energy 278 (2023) 127716, http://dx.doi.org/10.1016/j.energy.2023.127716, URL https://www.sciencedirect.com/science/article/pii/S0360544223011106.

[20] B.S. Palmintier, M.D. Webster, Impact of operational flexibility on electricity generation planning with renewable and carbon targets, IEEE Trans. Sustain. Energy 7 (2) (2016) 672–684, http://dx.doi.org/10.1109/TSTE.2015.2498640.

[21] International Renewable Energy Agency (IRENA), Socio-economic footprint of the energy transition: South africa, 2023, URL https://mc-cd8320d4-36a1-40ac-83cc-3389-cdn-endpoint.azureedge.net/-/media/Files/IRENA/Agency/Publication/2023/Nov/IRENA_Socio-economic_footprint_South_Africa_2023.pdf?rev=54c391f1dee54d0bbf78703db3e00145.

[22] A. Van Stiphout, K. Poncelet, K. De Vos, G. Deconinck, The impact of operating reserves in generation expansion planning with high shares of renewable energy sources, in: IAEE European Energy Conference, Sustainable Energy Policy and Strategies for Europe, Date: 2014/10/28-2014/10/31, Location: Rome, Italy, 2014, pp. 1–15.

[23] E. Giglio, D. Fioriti, [Stochasticmodelforreserveestimation], 2024, URL https://github.com/enricogiglio/StochasticModelforReserveEstimation.git.

[24] M. de la Torre Rodriguez, M. Scherer, D. Whitley, F. Reyer, Frequency Containment Reserves Dimensioning and Target Performance in the European Power System, IEEE, 2014, pp. 1–5, http://dx.doi.org/10.1109/PESGM.2014.6939825.

[25] T. Brown, J. Hörsch, D. Schlachtberger, PyPSA: Python for power system analysis, J. Open Res. Softw. 6 (4) (2018) http://dx.doi.org/10.5334/jors.188, arXiv:1707.09913.

[26] S. Boyd, L. Vandenberghe, Convex Optimization, Cambridge University Press, Cambridge, UK, 2004, URL https://web.stanford.edu/boyd/cvxbook/.

[27] M. Esmaili, M. Ghamsari-Yazdel, N. Amjady, C.Y. Chung, A.J. Conejo, Transmission expansion planning including tcscs and sfcls: A minlp approach, IEEE Trans. Power Syst. 35 (6) (2020) 4396–4407, http://dx.doi.org/10.1109/TPWRS.2020.2987982.

[28] M. Petrelli, D. Fioriti, A. Berizzi, D. Poli, Multi-year planning of a rural microgrid considering storage degradation, IEEE Trans. Power Syst. 36 (2) (2021) 1459–1469, http://dx.doi.org/10.1109/TPWRS.2020.3020219.

[29] Eskom, [Eskom data portal], 2023, URL https://www.eskom.co.za/dataportal/. (Accessed 01 December 2023).

[30] J. Horsch, J.R. Calitz, Pypsa-za: Investment and operation co-optimization of integrating wind and solar in south africa at high spatial and temporal detail, ArXiv: Phys. Soc. (2017) URL https://api.semanticscholar.org/CorpusID:62828063.

[31] H. Hersbach, B. Bell, P. Berrisford, S. Hirahara, A. Horányi, J. Muñoz-Sabater, J. Nicolas, C. Peubey, R. Radu, D. Schepers, A. Simmons, C. Soci, S. Abdalla, X. Abellan, G. Balsamo, P. Bechtold, G. Biavati, J. Bidlot, M. Bonavita, G. De Chiara, P. Dahlgren, D. Dee, M. Diamantakis, R. Dragani, J. Flemming, R. Forbes, M. Fuentes, A. Geer, L. Haimberger, S. Healy, R.J. Hogan, E. Hólm, M. Janisková, S. Keeley, P. Laloyaux, P. Lopez, C. Lupu, G. Radnoti, P. de Rosnay, I. Rozum, F. Vamborg, S. Villaume, J.-N. Thépaut, The era5 global reanalysis, Q. J. R. Meteorol. Soc. 146 (730) (2020) 1999–2049, http://dx.doi.org/10.1002/qj.3803, arXiv:https://rmets.onlinelibrary.wiley.com/doi/pdf/10.1002/qj.3803 URL https://rmets.onlinelibrary.wiley.com/doi/abs/10.1002/qj.3803.

[32] Republic of South Africa, Government gazette (42483) of 2019, 2019, URL https://www.treasury.gov.za/public%20comments/CarbonTaxBill2019/Carbon%20Tax%20Act%202019-Act%2015%20of%202019.pdf. (Accessed 13 June 2024).

[33] M. Economics, Review of the irp 2023, 2024, https://meridianeconomics.co.za/wp-content/uploads/2024/03/IRP2023-Modelling-Submission-20240318.0.pdf. (Accessed 05 May 2024).

[34] C. Auret, B. Bekker, Impact of partial unplanned outage modeling assumptions on long-term capacity planning validation, IEEE Access 12 (2024) 177427–177441, http://dx.doi.org/10.1109/ACCESS.2024.3506038.

[35] D. Banks, J. Schäffler, The potential contribution of renewable energy in south africa, 2006, Accessed 31 December 2023.

[36] Q. Han, Z.L. Liu, S.L. Liu, N. Xu, Analysis on operation reliability of wind power units in china, IOP Conf. Ser.: Earth Environ. Sci. 354 (1) (2019) 012034, http://dx.doi.org/10.1088/1755-1315/354/1/012034.

[37] S. Bofinger, B. Zimmermann, A.-K. Gerlach, Wind and solar pv resource aggregation study for south africa, 2016, URL https://www.csir.co.za/sites/default/files/Documents/Wind%20and%20Solar%20PV%20Resource%20Aggregation%20Study%20for%20South%20Africa_Final%20report.pdf.

[38] Q. Han, Z.L. Liu, S.L. Liu, N. Xu, Analysis on operation reliability of wind power units in china, IOP Conf. Ser.: Earth Environ. Sci. 354 (2019) 012034, http://dx.doi.org/10.1088/1755-1315/354/1/012034.

[39] T.-C. Kuo, T.T. Pham, D.M. Bui, P.D. Le, T.L. Van, P.-T. Huang, Reliability evaluation of an aggregate power conversion unit in the off-grid pv-battery-based dc microgrid from local energy communities under dynamic and transient operation, Energy Rep. 8 (2022) 5688–5726, http://dx.doi.org/10.1016/j.egyr.2022.03.190, URL https://www.sciencedirect.com/science/article/pii/S2352484722007454.

[40] L. Popp, K. Müller, Technical reliability of shipboard technologies for the application of alternative fuels, Energy Sustain. Soc. 11 (2021) 11–23, http://dx.doi.org/10.1186/s13705-021-00301-9.

[41] Republic of South Africa, Government gazette (49974) of 2024. integrated resource plan 2023, 2024, URL https://www.dmre.gov.za/Portals/0/Energy_Website/IRP/2023/IRP%20Government%20Gazzette%202023.pdf.

[42] C. Carà, P. Marocco, R. Novo, M. Koivisto, M. Santarelli, G. Mattiazzo, Modeling the long-term evolution of the italian power sector: The role of renewable resources and energy storage facilities, Int. J. Hydrog. Energy 59 (2024) 1183–1195, http://dx.doi.org/10.1016/j.ijhydene.2024.01.358, URL https://www.sciencedirect.com/science/article/pii/S0360319924003987.

[43] N. Kern, T. Gorgian, B. Nguyen, S. Damba, P. Moodley, P. Rambau, N. Sigwebela, Supply-side cost and performance data for eskom integrated resource planning: 2020–2021, 2021, update. EPRI.

[44] International Renewable Energy Agency (IRENA), Renewable energy prospects: South africa, 2020, URL https://www.irena.org/-/media/Files/IRENA/Agency/Publication/2020/Jun/IRENA_REmap_South_Africa_report_2020.pdf.

[45] M. Parzen, H. Abdel-Khalek, E. Fedotova, M. Mahmood, M.M. Frysztacki, J. Hampp, L. Franken, L. Schumm, F. Neumann, D. Poli, A. Kiprakis, D. Fioriti, Pypsa-earth, a new global open energy system optimization model demonstrated in africa, Appl. Energy 341 (2023) 121096, http://dx.doi.org/10.1016/j.apenergy.2023.121096, URL https://www.sciencedirect.com/science/article/pii/S0306261923004609.

[46] P. Marocco, R. Novo, A. Lanzini, G. Mattiazzo, M. Santarelli, Towards 100% renewable energy systems: The role of hydrogen and batteries, J. Energy Storage 57 (2023) 106306, http://dx.doi.org/10.1016/j.est.2022.106306, URL https://www.sciencedirect.com/science/article/pii/S2352152X22022952.

[47] W. Zeng, J. Fan, W. Zhang, Y. Li, B. Zou, R. Huang, X. Xu, J. Liu, Whole life cycle cost analysis of transmission lines using the economic life interval method, Energies 16 (23) (2023) http://dx.doi.org/10.3390/en16237804, URL https://www.mdpi.com/1996-1073/16/23/7804.

[48] M. Poller, M. Obert, G. Moodley, Analysis of Options for the Future Allocation of Pv Farms in South Africa, Study Report published by Deutsche Gesellschaft für Internationale Zusammenarbeit (GIZ) GmbH, 2015, URL https://www.sagen.org.za/publications/power-system-planning-operation/67-analysis-of-options-for-the-future-allocation-of-pv-farms-in-south-africa/file.

[49] International Renewable Energy Agency (IRENA), Innovation landscape brief: Flexibility in conventional power plants, 2019, URL https://www.irena.org/-/media/Files/IRENA/Agency/Publication/2019/Sep/IRENA_Flexibility_in_CPPs_2019.pdf?la=en&hash=AF60106EA083E492638D8FA9ADF7FD099259F5A1.

[50] C. van Dongen, B. Bekker, A. Dalton, Valuation of pumped storage in capacity expansion planning—a south african case study, Energies 14 (21) (2021) http://dx.doi.org/10.3390/en14216999, URL https://www.mdpi.com/1996-1073/14/21/6999.

[51] J. Jenkins, Z. Zhou, R. Ponciroli, R. Vilim, F. Ganda, F. de Sisternes, A. Botterud, The benefits of nuclear flexibility in power system operations with renewable energy, Appl. Energy 222 (2018) 872–884, http://dx.doi.org/10.1016/j.apenergy.2018.03.002, URL https://www.sciencedirect.com/science/article/pii/S0306261918303180.

[52] J. Usaola, Participation of csp plants in the reserve markets: A new challenge for regulators, Energy Policy 49 (2012) 562–571, http://dx.doi.org/10.1016/j.enpol.2012.06.060, URL https://www.sciencedirect.com/science/article/pii/S0301421512005708, special Section: Fuel Poverty Comes of Age: Commemorating 21 Years of Research and Policy.

[53] M. Świerczyński, D.I. Stroe, R. Lærke, A.I. Stan, P.C. Kjær, R. Teodorescu, S.K. Kær, Field experience from li-ion bess delivering primary frequency regulation in the danish energy market, ECS Trans. 61 (37) (2014) 1, http://dx.doi.org/10.1149/06137.0001ecst.

[54] C. Chardonnet, L. De Vos, F. Genoese, G. Roig, T. Bart, F. De Lacroix, T. Ha, B. Van Genabet, Study on Early Business Cases for H2 in Energy Storage and more Broadly Power to H2 Applications, Techinical Report: P2H-BC/4NT/0550274/000/03, 2017, URL https://www.h2knowledgecentre.com/content/researchpaper1130.

[55] E. Giglio, R. Novo, G. Mattiazzo, D. Fioriti, Reserve provision in the optimal planning of off-grid power systems: Impact of storage and renewable energy, IEEE Access 11 (2023) 100781–100797, http://dx.doi.org/10.1109/ACCESS.2023.3313979.

[56] E. Rozzi, E. Giglio, C. Moscoloni, R. Novo, G. Mattiazzo, A. Lanzini, Comparative study of electric and hydrogen mobility infrastructures for sustainable public transport: A pypsa optimization for a remote island context, Int. J. Hydrog. Energy 80 (2024) 516–527, http://dx.doi.org/10.1016/j.ijhydene.2024.07.105, URL https://www.sciencedirect.com/science/article/pii/S0360319924027769.

[57] Eskom, Pumped storage generating hours, gas generation and manual load reduction, 2023, URL https://www.eskom.co.za/dataportal/supply-side/pumped-storage-generating-hours-gas-generation-and-manual-load-reduction/.

[58] Eskom, Peaking power stations, 2023, URL https://www.eskom.co.za/eskom-divisions/gx/peaking-power-stations/.